Tectonophysics 524–525 (2012) 59–75

Contents lists available at SciVerse ScienceDirect

Tectonophysics

journal homepage: www.elsevier.com/locate/tecto

Intraplate Late Jurassic deformation and exhumation in western central Argentina: Constraints from surface data and U–Pb detrital zircon ages

Maximiliano Naipauer [a,*], Ezequiel García Morabito [a,b], Juliana C. Marques [c], Maisa Tunik [b,d], Emilio A. Rojas Vera [b], Graciela I. Vujovich [a,b], Marcio P. Pimentel [c], Victor A. Ramos [a,b]

[a] Instituto de Estudios Andinos "Don Pablo Groeber", Departamento de Ciencias Geológicas, FCEN, Universidad de Buenos Aires, Argentina
[b] CONICET, Argentina
[c] Laboratorio de Geología Isotópica, Universidade Federal do Rio Grande do Sul, Brazil
[d] Instituto de Investigación en Paleobiología y Geología, Sede Alto Valle, Universidad Nacional de Río Negro, Argentina

ARTICLE INFO

Article history:
Received 10 August 2011
Received in revised form 3 December 2011
Accepted 10 December 2011
Available online 22 December 2011

Keywords:
Neuquén basin
Intraplate deformation
Weakness zone
Detrital zircons
Provenance
Huincul high

ABSTRACT

Intraplate deformation has been described in several tectonic settings and recently in western central Argentina it has been proposed to explain the complex structural patterns developed between Early Jurassic and Cretaceous times along the Huincul deformation zone. We integrate new field data and detrital zircon ages of the exposed portion of the Huincul High that permit us to quantify the significance of this intraplate deformation in the relief generation. A stratigraphic and structural record of a Jurassic pulsed contractional deformation is derived from field surveys. It is documented through multiple unconformities and growth geometries linked to NE and E–W oriented growth structures extensively developed across the studied region. The pattern of zircon ages from the analyzed Late Jurassic successions indicates that they have a clear provenance from sources located along the Huincul deformation zone. The Tordillo Formation outcrops north of the Huincul High have a dominant provenance from the Andean Jurassic arc; while the Quebrada del Sapo Formation, south of the Huincul High, has a significant input from Late Triassic (220–200 Ma) and Late Permian (280–260 Ma) sources of the axial exposures of the Huincul High. Surface data, combined with detrital zircon ages proved to be a powerful method to confirm the presence of an ancient positive element developed within the southern Neuquén basin. Its genesis falls within the early history of the Huincul deformation zone, where several structural features indicate pulses of growth since Early Jurassic times prior to the main Andean contractional cycle that started in the Late Cretaceous. Therefore, these data document for the first time the importance of the early contractional phases in the relief construction in the southern Central Andes, reinforcing previous hypotheses about pre-Andean intraplate deformation concentrated along this extensive east–west oriented basement weakness zone.

1. Introduction

Intraplate deformation has been described in several tectonic scenarios around the world. Although most of the documented cases occur in the hinterland and foreland areas of collisional orogens, it may also take place within Andean-type orogens (Storti et al., 2003; Ziegler et al., 1995, 1998).

In western central Argentina, intraplate deformation has been recently proposed to explain the complex structural patterns developed between Early Jurassic and Cretaceous times along an extensive east–west oriented basement weakness zone linked to the amalgamation of Patagonia to the rest of Gondwana in late Paleozoic times (Chernicoff and Zappettini, 2004; Mosquera and Ramos, 2006; Mosquera et al., 2011; Ramos, 2010). This corridor of deformation defines a regional first-order morphostructural feature best known as the Huincul High (Fig. 1). It extends for hundreds of kilometers towards the foreland, truncating the entire Neuquén Basin. This is a major petroleum province in Argentina located in the eastern foothills of the Andes between 32° and 41°S, where thousands of meters of Mesozoic sedimentary successions accumulated under the combined effects of sea-level changes, tectonic activity, and varying subsidence rates (Gulisano and Gutiérrez Pleimling, 1995; Howell et al., 2005; Vergani et al., 1995).

Several studies carried out by the oil companies along the Huincul zone documented persistent tectonic activity associated with the growth of structures and uplift that began in the Early Jurassic and lasted practically until the Cretaceous (García Morabito, 2010; Mosquera and Ramos, 2006; Orchuela et al., 1981; Pángaro et al., 2009; Ploszkiewicz et al., 1984; Silvestro and Zubiri, 2008; Vergani et al., 1995). This intraplate deformation was interpreted as a being the result of the interface between basement anisotropies, plate convergence directions, and strain

* Corresponding author. Tel.: +54 11 48273216.
E-mail address: maxinaipauer@gl.fcen.uba.ar (M. Naipauer).

0040-1951/$ – see front matter © 2011 Elsevier B.V. All rights reserved.
doi:10.1016/j.tecto.2011.12.017

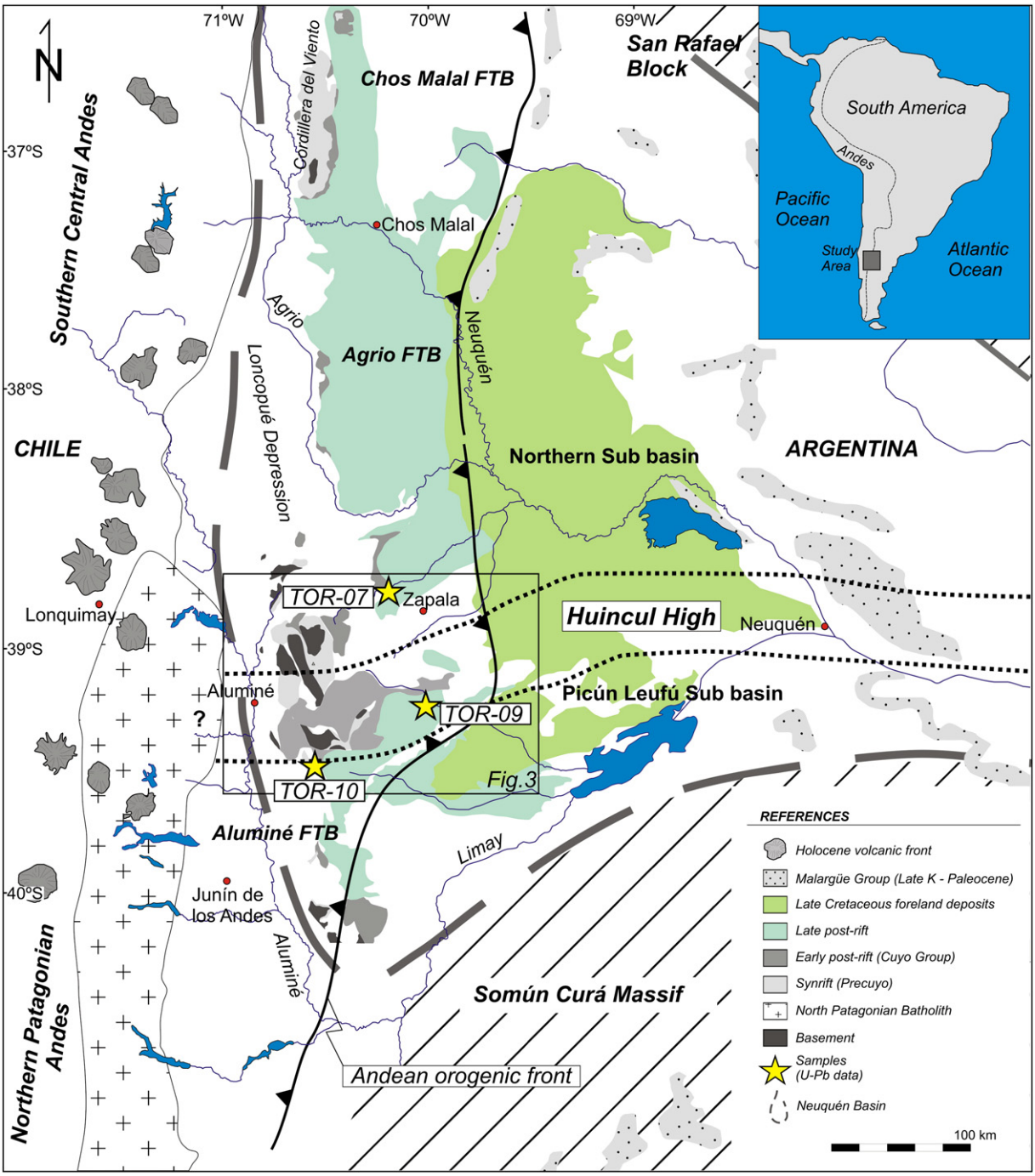

Fig. 1. Generalized tectonic map of the Neuquén Basin with distribution of the basin deposits and indication of sample localities in the area of influence of the western Huincul High.

orientations (Mosquera and Ramos, 2006). The inception of the Early Jurassic deformation was specifically a consequence of the conjunction of an east–west trending weakness zone and NW to NNW directed stresses, consistent with the convergence direction between the Aluk oceanic plate and the Gondwana continental margin during that time.

Complementary sedimentological studies inferred that the Huincul High formed an ancient positive element which acted as a structural and stratigraphic barrier at least during the Late Jurassic, participating as a potential source area for the Neuquén Basin at that time, and dividing the basin in two depocenters (Gulisano, 1988; Marchese, 1971; Spalletti and Colombo, 2005; Spalletti et al., 2008; Vergani et al., 1995; Zavala et al., 2005).

According to the known paleogeography, the northeastern and southwestern margins of the Neuquén Basin, represented by the San Rafael Block and the Somún Curá Massif respectively, as well as its western margin defined by an almost continuous volcanic arc, could also have acted as positive source areas that drained to the basin (Fig. 1). However, no information is available on the relative importance of each of these sectors as source areas during the early stages of development of the Huincul High as a potential positive element. There is also a lack of information about the real extent and importance of these early contractional phases in the relief construction along this intraplate deformation zone, and consequently about the extension of the potentially exhumed foreland areas and its role in the Late Jurassic paleography of the basin.

This work combines field data from the western portion of the Huincul High, combined with LAM–MC–ICP–MS U–Pb detrital zircon ages. Late Jurassic representative samples collected from the area of

influence of the Huincul High were studied in order to establish a potential relationship between intraplate deformational pulses and potentially exhumed areas located along the Huincul High during Jurassic times. The integration of these data represents a powerful method to evaluate possible uplift pulses along the Huincul deformation zone, to establish ages of the exhumed source areas as well as to quantify their importance in the growth of the proto-Andean orogen.

2. Geologic and tectonic setting

The Neuquén Basin, located along the eastern foothills of the Andes from 32° to 41°S, contains several thousand meters of Late Triassic to Early Cretaceous marine and continental sequences accumulated on the eastern side of the Andean volcanic arc under variable sedimentary and tectonic conditions (Fig. 2). The tectonic evolution of the basin records a complex history that includes a Late Triassic–Early Jurassic rift stage, followed by a long period of thermal sag (Middle Jurassic to earliest Cretaceous) and a Late Cretaceous–Cenozoic foreland stage (Franzese and Spalletti, 2001; Howell et al., 2005; Vergani et al., 1995).

The basin is strongly influenced by a first-order morphostructural feature known as the Huincul High (de Ferraríis, 1947). This is an east–west oriented positive element which extends towards the foreland for more than 270 km, conforming a structural and stratigraphic barrier that divides the Neuquén Basin into two main depocenters or sub-basins (Mosquera and Ramos, 2006; Zavala et al., 2005) (Fig. 1). Several studies carried out by the oil companies during recent decades resulted in a robust knowledge of its stratigraphic and structural configuration (Grimaldi and Dorobek, 2011; Mosquera and Ramos, 2006; Orchuela et al., 1981; Pángaro et al., 2006; Pángaro et al., 2009; Ploszkiewicz et al. 1984; Silvestro and Zubiri, 2008; Vergani et al., 1995, among others), although controversies about the mechanisms of deformation still persist. Its complex structural configuration resulted from the interaction between a series of WNW to NW-trending extensional faults of the rift phase, and subsequent deformational pulses which affected the entire system and resulted in compressive and transpressive structures of variable orientation (García Morabito, 2010; Pángaro et al., 2009; Silvestro and Zubiri, 2008).

The study area covers the northern and southern flanks of the western portion of the Huincul High, which corresponds to the segment that is better exposed at the surface (Fig. 3). In this region, the metamorphic and igneous basement and the Mesozoic sedimentary fill of the basin crop out over a wide area as a result of successive deformational events which affected the region. The basement is dominated by metasedimentary rocks included in the Piedra Santa Formation and Colohuincul Complex (Franzese, 1995; Turner, 1973) and Late Paleozoic igneous rocks.

A maximum depositional age of ~364 Ma has been established with U–Pb analyses in detrital zircons of the Piedra Santa phyllites and schists exposed in the "Cuesta de Rahue" at the western margin of the study area (Ramos et al., 2010). Franzese (1995) also obtained K/Ar (whole rock) ages which yielded values between 372 and 311 Ma, identifying a late Paleozoic age for the metamorphism. Similar ages were reported by Lucassen et al. (2004) in migmatites exposed farther south, where they obtained ages of 380 ± 2 Ma ($^{206}Pb/^{238}U$) and 375 ± 15 Ma ($^{207}Pb/^{235}U$) in titanites, interpreting them as the age of crystallization of this mineral.

Igneous rocks comprise calc-alkaline tonalites and granodiorites that constitute the core of the main topographic features across the study area. A K–Ar (biotite) age of 281 ± 4 Ma for a porphyry of tonalitic composition next to Cerro Chachil was reported by Sillitoe

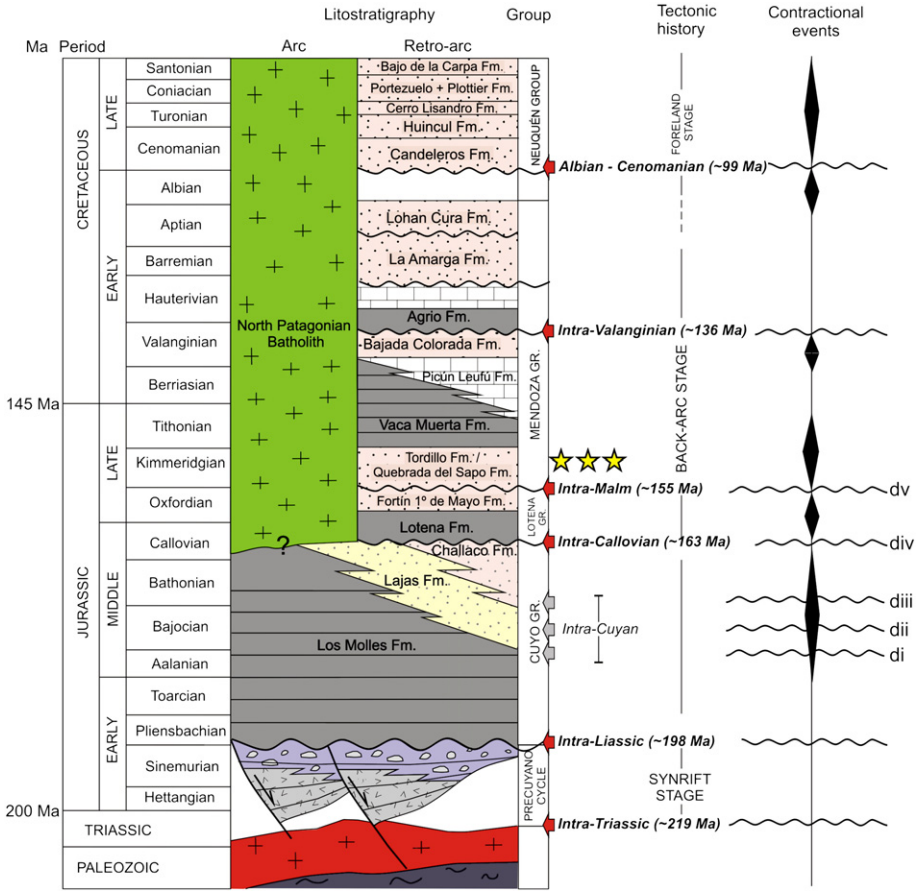

Fig. 2. Tectonostratigraphic chart of the southern Neuquén Basin and adjacent sectors showing main unconformities, timing of deformation, and stratigraphic location of the studied samples.

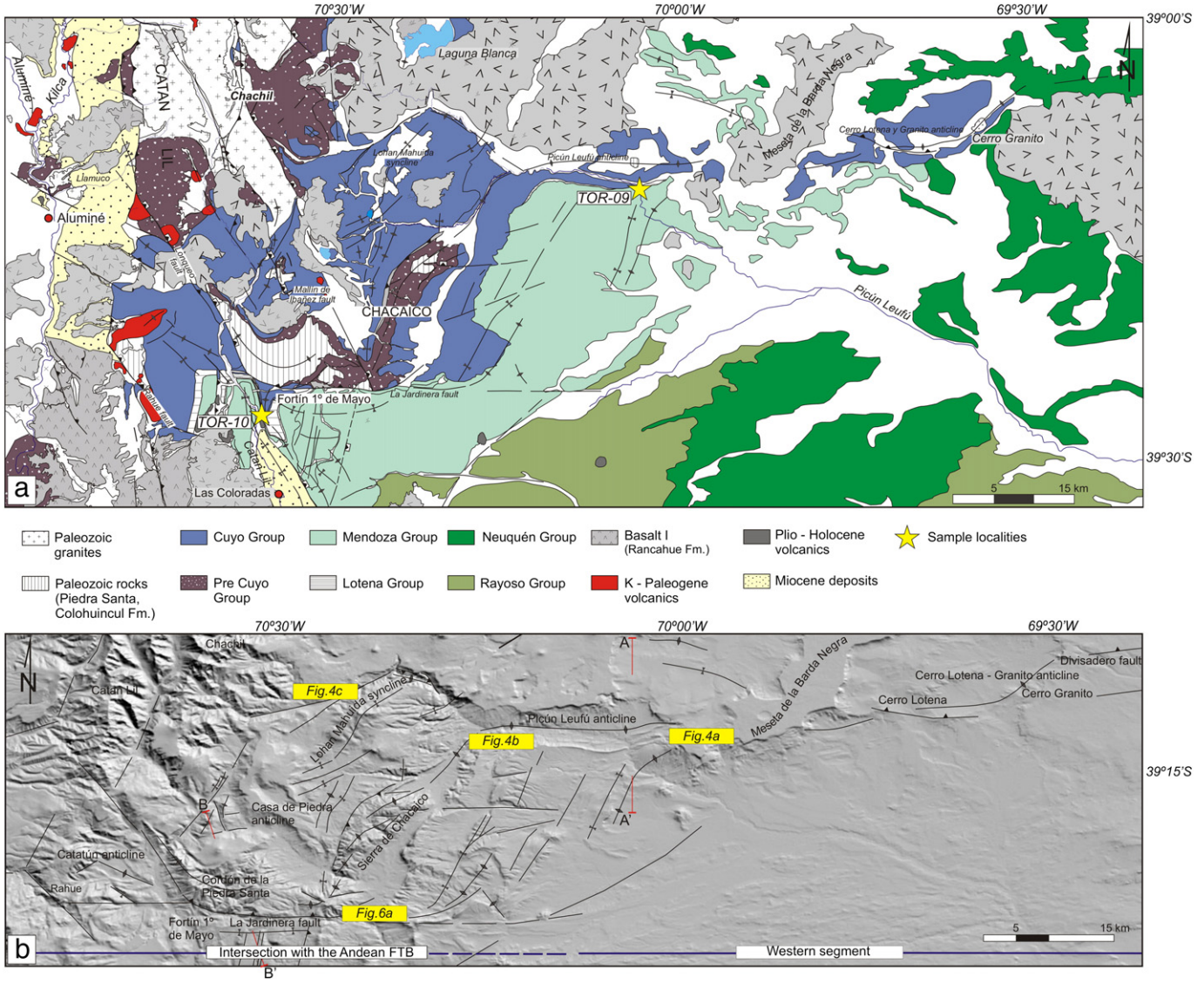

Fig. 3. Geological and structural map of the western Huincul High. a) Geological map of the western Huincul arch and its area of influence where it intercepts the Andean fold and thrust belt (modified from Leanza and Hugo (1997) and García Morabito et al. (2011)). b) Main structural elements associated with the exposed segment of the Huincul High.

(1977). Single zircon ages from hydrocarbon well cores of the western portion of Huincul High indicate ages of 286.5 ± 2.3 Ma and 284.0 ± 1.3 Ma for a granodiorite and an andesitic dike, respectively (Schiuma and Llambías, 2008). Older ages were obtained south of the study area by Lucassen et al. (2004), who reported Rb–Sr ages of 299 ± 6 and 299 ± 7 Ma in diorites exposed between Junín de los Andes and Rahue.

The informal term pre-Cuyo or Precuyano Cycle, is commonly used to the volcano-sedimentary sequences located stratigraphically between the basement and the lowest marine sediments of the Cuyo Group (Gulisano et al., 1984), which were deposited in a series of fault-bounded isolated half grabens heterogeneously distributed along the region during Late Triassic – Early Jurassic times (Franzese and Spalletti, 2001; Vergani et al., 1995). The synrift volcanic infill that constitutes the lower section of the Precuyano Cycle mainly consists of andesites, rhyolites and volcaniclastic deposits. A series of siliciclastic facies with significant pyroclastic components represent its upper section (Franzese et al., 2006; García Morabito, 2010; Leanza et al., 2005; Legarreta and Gulisano, 1989). Absolute ages of the synrift strata in the study and neighbouring areas range between 219 Ma and 182 Ma (Franzese et al., 2006; Pángaro et al., 2002; Rapela et al., 1983; Schiuma and Llambías, 2008).

The pre-Cuyo strata underlie thousands of meters of a postrift succession deposited during three principal transgressive–regressive cycles. The marine Cuyo Group successions represent the first of these cycles and comprise three major sequences deposited during Pliensbachian–Bathonian times that include deep marine shales (Los Molles Formation), shallow-marine to deltaic deposits (Lajas Formation), and fluvial deposits (Challacó Formation). A regional unconformity (Intra-Callovian ~155 Ma) separates these sequences from the Lotena Group successions (Leanza, 2009), consisting of deltaic to shallow-marine deposits represented by conglomerates, sandstones and shales included in the Lotena Formation, and continental sandstones and conglomerates deposited in a fluvial environment corresponding to the Fortín 1° de Mayo Formation (Cucchi et al., 2005, Gulisano et al., 1984; Leanza, 1990, 1993).

A new sedimentation cycle is represented by hundred of meters of the Mendoza Group. It comprises several units documenting a period of basin expansion throughout the retroa-arc region. These include the Tordillo and Quebrada del Sapo Formations, represented by sandstones and conglomerates accumulated in fluvial and littoral environments during the Kimmeridgian. These units are covered by richly fossiliferous Tithonian marine dark shales of the Vaca Muerta Formation, which represents an important transgression well documented by the ammonite

fauna along the entire basin (Gulisano and Gutiérrez Pleimling, 1995; Leanza, 1981; Riccardi, 2008a,b; Vergani et al., 1995). Fine-grained strata are gradually replaced by shallow-marine limestones of the Picún Leufú Formation (Leanza and Hugo, 1997) and by continental sediments of the Bajada Colorada Formation. Finally, the near-shore Early Cretaceous Agrio Formation completes the stratigraphic record of this group.

Barremian–Albian evaporites and clastic sedimentary rocks are represented by the La Amarga and Lohan Cura Formations (Leanza and Hugo, 1997), exposed northeast and southeast of the study area. The final continentalization of the basin is marked by the conglomerates, sandstones and shales of the Late Cretaceous Neuquén Group.

The Mesozoic units crop out over a wide area in the limbs of broad anticlinal structures that define the western portion of the Huincul High and constitute the main topographic features across the region (Fig. 3).

3. Structural configuration and onset of deformation

The Huincul High constitutes an east–west oriented morphostructural feature developed within a basement weakness zone linked to the amalgamation of Patagonia to the rest of Gondwana by the end of the Paleozoic (Mosquera and Ramos, 2006; Ramos, 2008, 2010). This ancient positive element is formed by a set of structures which extend at depth for hundreds of kilometers across the entire Neuquén Basin, reaching the foothills of the Northern Patagonian Andes. The interaction between a series of normal faults of the early Mesozoic rift phase and subsequent contractional pulses resulted in a complex structural framework given by a set of structures of different trends and behaviors (García Morabito, 2010; Grimaldi and Dorobek, 2011; Pángaro et al., 2009; Silvestro and Zubiri, 2008).

Most of the structural studies of the Huincul High have been carried out by the oil industry since the early eighties, resulting in a robust knowledge of its subsurface configuration, mainly through the analysis of three-dimensional seismic cubes (Grimaldi and Dorobek, 2011; Mosquera and Ramos, 2006; Pángaro et al., 2009; Silvestro and Zubiri, 2008). The characterization of the principal structural features at depth allowed the recognition of different sectors: a western sector dominated by NE-rending anticlines, a central sector characterized by E–W oriented structures, and an eastern one where NW–trending lineaments predominate (Silvestro and Zubiri, 2008). Many of the studies carried out along this deformation zone at depth, agree in establishing a multiepisodic tectonic activity which started during the Toarcian, coeval with the deposition of the lower Cuyo Group, and persisted until the Cretaceous (Grimaldi and Dorobek, 2011; Mosquera and Ramos, 2006; Pángaro et al., 2009; Silvestro and Zubiri, 2008; Vergani et al., 1995). Studies from outcrops located around Cerro Lotena and Cerro Granito, where the western limit of the Huincul High is commonly established, resulted in similar conclusions (Vergani, 2005; Zavala et al., 2008; Zavala and Freije, 2002). In the Cenomanian, the Huincul High became less active, although some deformation continued into the Tertiary (Uliana et al., 1995; Mosquera and Ramos, 2006). Several unconformities mark these tectonic events along the Huincul High. They are referred to as the intra-Liassic, intra-Cuyan, intra-Callovian, intra-Malm, and intra-Valanginian (Fig. 2).

The Huincul High continues at surface into the foothills of the Patagonian Andes, where basement rocks and synrift sequences linked to a series of reverse faults and anticlines of variable orientation are exposed (Fig. 3a). This area, located west of the Cerros Lotena and Granito, constitutes its westernmost expression, and received little attention from a structural point of view compared to the well constrained (at depth) eastern sectors. Due to its particular evolution, which resulted in the exposure of the basement, synrift and early postrift successions in a close relationship with several east–west and NE-trending structures, this portion of the foreland constitutes a key area in which to evaluate the inception of the pre-Andean deformation.

3.1. Structural framework

This western segment records the superimposition of different structural styles as a consequence of the incorporation of the structural features related to the early development of the westernmost Huincul High into the Andean fold and thrust belt by the end of the Cretaceous (García Morabito, 2010; García Morabito and Ramos, 2011a,b) (Fig. 3). Structures developed during the Andean cycle were geometrically controlled not only by the presence of a series of NW to NNW-trending normal faults of the early Mesozoic rift phase (Franzese et al., 2006; García Morabito et al., 2011), but also by the trend of several pre-Andean contractional structures linked to the early history of the Huincul High. Interference resulted in an extremely complex structural framework, given by highly scattered structures with contrasting trend and vergence, and abrupt changes in their orientation (Fig. 3b).

This portion of the foreland provides good exposures of the synrift and basement rocks, recording a dramatic change in the structural relief compared with the neighboring northern and southern areas, where the basement and the synrift deposits are buried beneath several thousands of meters of Mesozoic sedimentary successions. Such latitudinal variations are accompanied by significant topographic and structural changes, and they are linked to a series of pre-Andean east–west oriented faults that conditioned the peculiar configuration of this foreland segment (Fig. 3). They comprise an ensemble of structural features which can be considered as the surface prolongation of the Huincul High to the west due to its orthogonal arrangement with respect to the Andean fold and thrust belt, and several evidences of its pre-Andean growth and development.

The structural framework of the western portion of the Huincul High can be described as being provided by three preferential trends of the main structural features which are NNW, NE, and E–W (Fig. 3). These features define a structural arrangement of similar characteristics with respect to those described at depth (Silvestro and Zubiri, 2008). Most of the NE-trending structures correspond to west-verging anticlines developed in the Mesozoic sequences, frequently related to high angle basement faults orthogonally arranged with respect to the NW to NNW-trending faults of the Upper Triassic–Lower Jurassic rift phase. E–W structures correspond to north dipping basement faults with important reverse and minor slip components, and to south-verging anticlines of regional extension (Figs. 3 to 6).

A series of growth strata and associated unconformities observed in the postrift sedimentary succession document a persistent Jurassic tectonic activity, which controlled the sedimentation along the axes of the westernmost portion of the Huincul High. These unconformities are recognized in different portions of the basin and specifically around the main structural features of the study area, where they reflect a local response to tectonism together with growth geometries, wedge geometries, thickness changes, erosional surfaces and breaks in the sedimentary record.

3.2. Sierra de Chacaico, La Jardinera fault, Picún Leufú anticline, and adjacent features

The Sierra de Chacaico, La Jardinera fault, and the Picún Leufú anticline (Fig. 3) represent the most conspicuous features within a set of structures which define a combined NE and E–W trend in map view. These are first-order regional structures which represent the surface expression of the western Huincul High. These structures also document the first pulses of deformation that affected this morphotectonic unit where it intercepts the Andean fold and thrust belt.

The Sierra de Chacaico corresponds to an asymmetric west-verging anticline linked to an east-dipping and NE-trending reverse

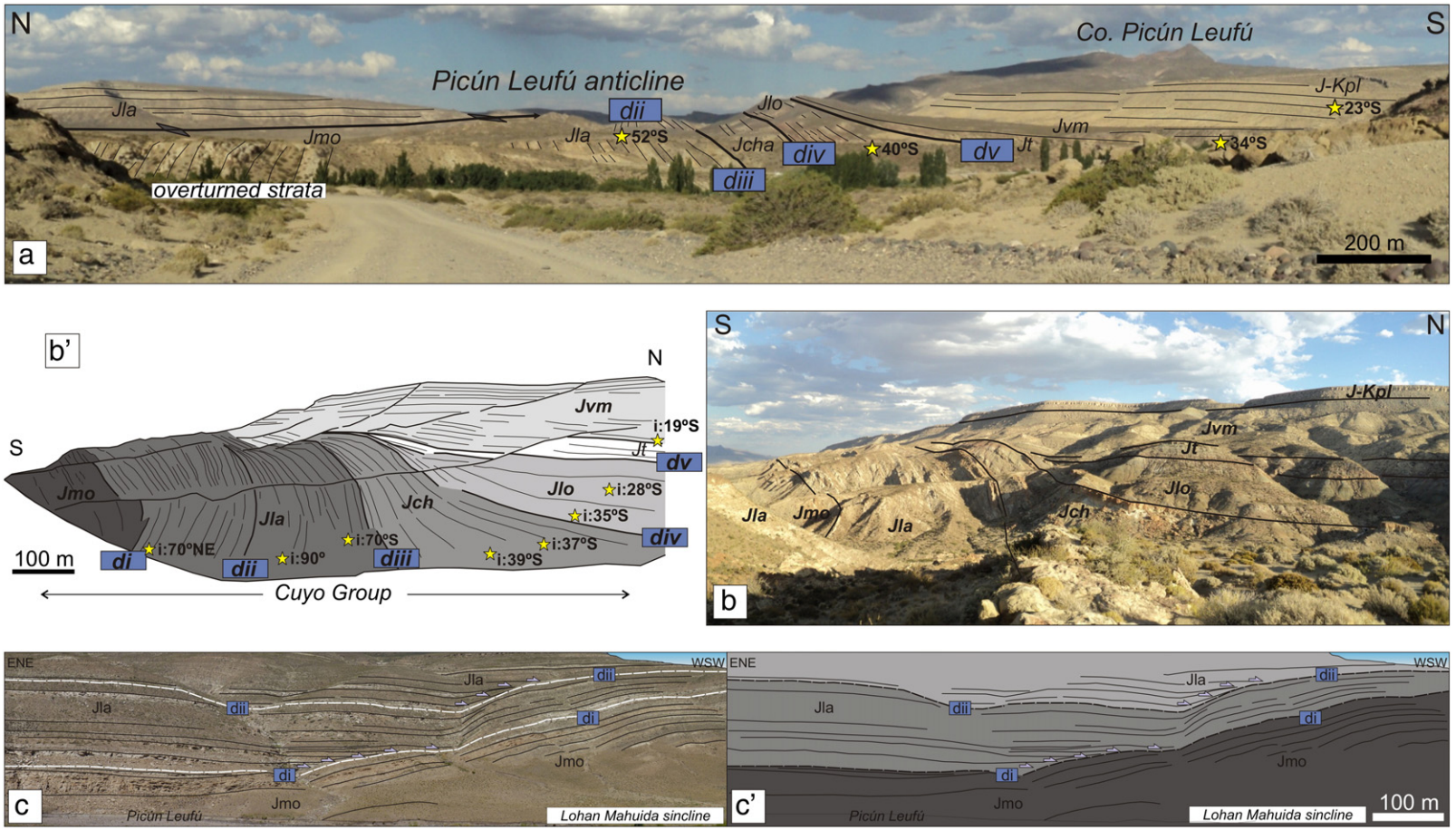

Fig. 4. Mesozoic growth structures across the western Huincul High: Picún Leufú anticline and Lohan Mahuida syncline, and field evidences for Jurassic onset in deformation. Abbreviations: Jmo—Los Molles Formation, Jla—Lajas Formation, Jcha—Challado Formation, Jlo—Lotena Formation, Jt—Tordillo Formation, Jvm—Vaca Muerta Formation, J-Kpl—Picún Leufú Formation. a) Eastward view of the south-verging Picún Leufú growth anticline. Older strata became progressively more overturned due to ongoing deformation. b) Photograph looking east at the occidental forelimb of the Picún Leufú anticline (modified from Leanza (2009)), and b′) line drawing and interpretation of the main recognizable bounding surfaces, unconformities, and growth geometries within the Jurassic successions. Stars indicate measured dip. c) Southeastward view of the western flank of the NE-trending Lohan Mahuida syncline, and c′) line drawing of bounding surfaces within the lower Cuyo Group successions. Note intra-cuyan unconformities and onlap relationships against these boundaries.

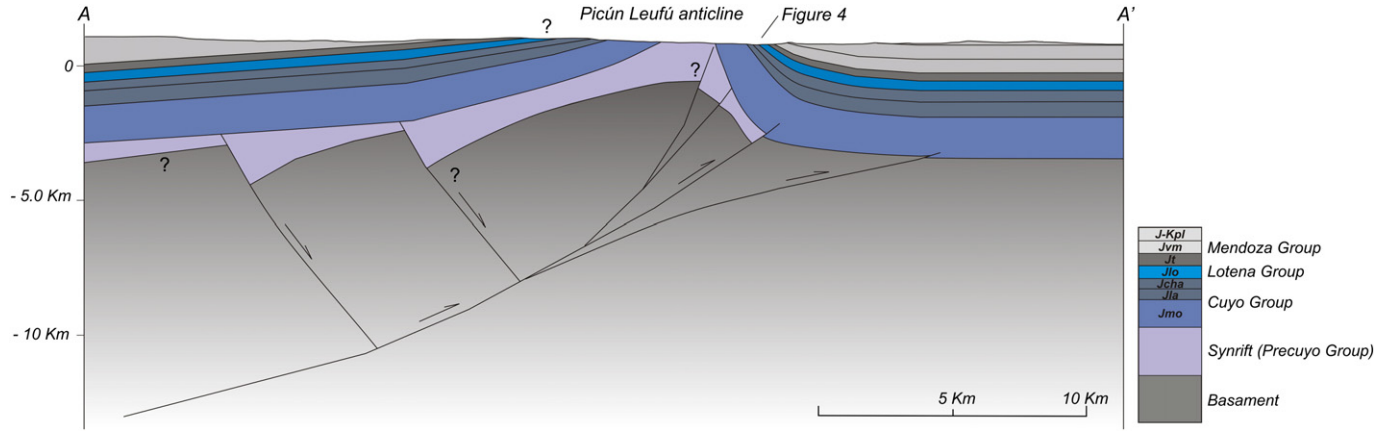

Fig. 5. North–south oriented geological cross section across the Picún Leufú anticline constructed on the basis of surface geology. The trace of the cross section is indicated in Fig. 3. Note growth wedge geometry at the anticline forelimb.

fault which reaches the surface along its western slope (Franzese et al., 2007; Leanza and Hugo, 1997). This topographic feature consists internally of three stepping NE-trending basement cored anticlines, which where uplifted in successive pulses to the west, providing good exposures of the basement and of the pre-Cuyo sequences as well. The Jurassic and Early Cretaceous Cuyo and Mendoza groups crop out along its entire eastern slope. Here, the dip of the different unconformity-bounded stratigraphic units gradually decreases towards the top of the sequence, showing growth geometries, truncation and onlap relationships at their boundaries.

East of the course of the Arroyo Chacaico, the Tordillo Formation unconformably overlies the successions of the Cuyo Group. This implies a break in the sedimentary record expressed by the absence of the Lotena Group successions in the area, due to a period of local non-deposition or erosion associated with deformation and uplift of this topographic feature. Anomalously reduced thicknesses or absence of some stratigraphic terms are common within the vicinity areas of the Huincul deformation zone, reflecting periods of uplift and low subsidence along its axis.

The main NE-trending fold axes of the Sierra de Chacaico area dramatically change their orientation to the north and to the south, where they intercept two regional east–west oriented structures represented by the Picún Leufú anticline and La Jardinera fault respectively (Fig. 3b).

The east–west oriented Picún Leufú anticline extends for more than 20 km parallel to the course of the river of the same name (Leanza and Hugo, 1997) (Fig. 3). Detailed stratigraphic studies were carried out in the area by Zavala and Freije (2002) and Zavala

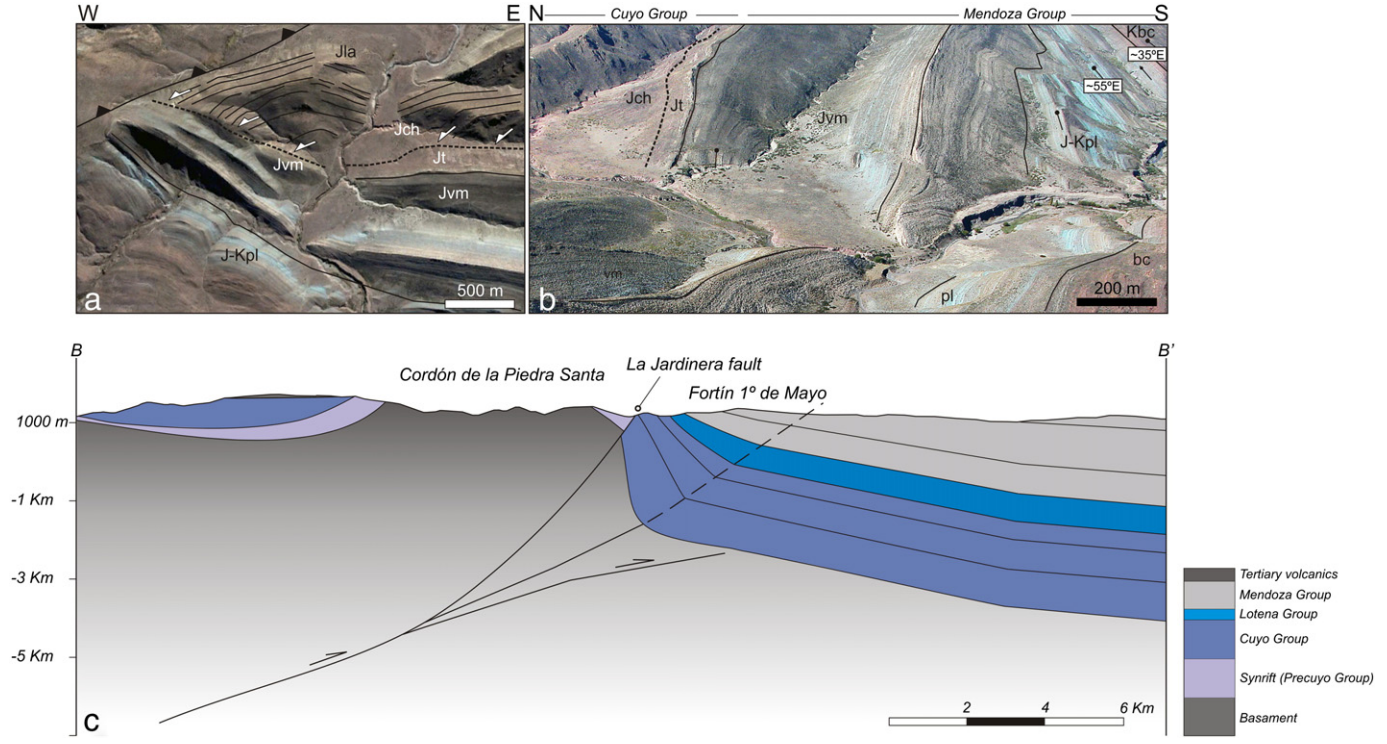

Fig. 6. Cordón de la Piedra Santa and La Jardinera fault. a) Field relationship between the Tordillo successions and the upper Cuyo Group sequences at the easternmost segment of La Jardinera fault. Note unconformity separating strata of the Tordillo Formation from rocks of the Challaco Formation; b) Photograph looking north of the Mendoza and Cuyo groups at the eastern La Jardinera fault. Note how the Late Jurassic–Late Cretaceous successions overstep the whole sequence (Photo by Jorge Amado). c) NNW–SSE oriented geological cross section across the Cordón de la Piedra Santa constructed on the basis of surface geology. The trace of the cross section is indicated in Fig. 3. Note growth wedge geometry at the football of La Jardinera fault.

et al. (2008). It constitutes a south-verging anticline that involves the sedimentary successions of the Cuyo, Lotena, and Mendoza groups, which were progressively folded and transported to the south. Pulsed tectonic activity is recorded throughout the entire Jurassic postrift succession which forms both limbs of the anticline. It is expressed by a complex array of growth unconformities and sedimentary wedges developed within the postrift successions (Fig. 4). Forelimb beds show a continuous variation from overturned to steep beds to almost flat lying strata at the top of the sequence (Figs. 4a and 5), indicating successive pulses of growth during a time interval comprised between the Toarcian and the Valanginian.

Fig. 4b illustrates the western portion of the anticline forelimb which is particularly valuable for the analysis of the growth geometries. The dip of the Cuyo Group successions progressively decreases from steeply overturned to shallowly-dipping strata across the western portion of the frontal limb. The different dip domains are bounded by several growth unconformities (di, dii, diii, and div), indicating that sedimentation was coeval with both subsidence and contractional deformation. Their expression gradually disappears towards the north where the influence of the Huincul deformational zone decreases (Leanza, 2009). Substantial thickening of stratigraphic units occur northwards across the anticline forelimb. Thickness variation is particularly well expressed in strata of the Challaco Formation, which thin markedly against the steep limb, overlapping surface div. Above this unit, marine strata of the Lotena Formation progressively onlaps and eventually overlaps surface div, showing notable thickening northwards from the fold axis. They are in turn unconformably covered by the Tordillo Formation sequences, which also record thickness variation and growth onlap. Towards the top, gently dipping Tithonian mudstones of the Vaca Muerta Formation and limestones of the Picún Leufú Formation successively overstep the whole sequence.

Similar evidences are observed several kilometers west and east of the Picún Leufú anticline. Its eastern prolongation corresponds to the east–west to NE oriented basement cored anticline of Cerro Lotena and Cerro Granito (Fig. 3). Structural relationships across the forelimb of this south-verging anticline, show a progressive decrease in dip of the Mesozoic successions which are in turn bounded by several unconformities (Mosquera, 2008; Vergani, 2005; Zavala and Freije, 2002). In this area, a principal unconformity separates the overturned to vertical strata of the Lajas Formation, from the north dipping sequences of the Lotena Group, which are in turn unconformable covered by gently dipping marine mudstones of the Vaca Muerta Formation (Mosquera, 2008; Vergani, 2005; Zavala and Freije, 2002). Flat-lying Cenomanian red beds of the Neuquén Group cover the whole succession. Kimmeridgian strata of the Tordillo Formation are absent across the area, due to its erosion or non-deposition.

Evidences of early deformation also come from the occurrence of growth unconformities and thickness changes across the western flank of the NE-trending Lohan Mahuida anticline, located several kilometers west of the Sierra de Chacaico (Figs. 3 and 4c). Here, the Jurassic successions of the Cuyo Group which conform its western flank appear bounded by two minor intra-Cuyan growth unconformities (di and dii). To the east, both unconformities abruptly become bedding-parallel. Surface di separates NE dipping strata of the Los Molles Formation from onlapping strata of the lower Lajas Formation, which also record thickness changes within the limb. The second surface lies within the Lajas Formation. Above this level, gently dipping strata progressively onlaps and eventually overlaps surface dii (Fig. 4c).

La Jardinera fault is an east–west oriented and south-verging reverse fault which falls into a transverse regional lineament identified as Las Coloradas–Villarrica on both sides of the Andean chain (Chotin, 1976). East of Fortín 1° de Mayo, it bounds the southern slope of the Cordón de la Piedra Santa, which constitutes a basement cored south-verging anticline that strongly affected the Mesozoic successions that crop out immediately to the south (Fig. 6). The uplift of this topographic element as a south-verging block was responsible for the overlapping of the Cuyo Group sequences with the metamorphic basement and synrift successions, and for the overturning of the Mesozoic successions along the faults trace (Fig. 6). The dip of the Mesozoic strata accumulated in the footwall show a continuous variation from overturned to shallow dipping to flat lying strata at the top of the sequences, and are in turn bounded by multiple unconformities. Jurassic strata thin toward the north as they approach the fault trace, defining a growth wedge geometry at the footwall (Fig. 6c).

The early uplift of the Cordón de la Piedra Santa is also evidenced by a discontinuity which directly juxtaposes the Tordillo Formation over the strata of the Challaco Formation next to the easternmost portion of the La Jardinera fault (Fig. 6a and b). This break in the sedimentary record implies the absence of the Callovian stratigraphic terms of the Lotena Group, suggesting its complete local erosion due to uplift of this regional structure prior to the deposition of the Tordillo Formation.

3.3. Onset of deformation

As a whole, structural and stratigraphical mapping constrains the inception of Jurassic deformation in the area through a series of unconformities and preserved growth geometries which reflect persistent periods of uplift and low subsidence.

Intra-Cuyan unconformities (di, dii, and diii) are the result of early tectonism in the area. They indicate that sedimentation was coeval with both subsidence and contractional deformation. Their influence gradually disappears towards the north where the control of the Huincul High decreases (Leanza, 2009). The intra-Callovian and intra-Malm unconformities mark significant subsequent tectonic events, probably occurred during the deposition of the Challaco and the Lotena Formations, as deduced from the occurrence of thickness changes, breaks in the sedimentary record, and growth geometries within the time interval represented by both units.

This complex array of unconformities and growth geometries document the early development of several NE and east–west oriented growth structures which define the exposed segment of the Huincul deformational zone. Along these basement cored structures, the first pulses of deformation predate the Kimmeridgian, when the deposition of the Tordillo Formation and equivalent units took place.

Detailed stratigraphic surveys across the area further confirm the presence of emerged areas along the western Huincul High which acted as structural and stratigraphic barriers. These areas supplied the sediments eroded from the uplifted Jurassic strata north and south of its axis, with paleocurrents from the N–NE, and from the SW respectively (Gulisano, 1988; Spalletti and Colombo, 2005; Zavala and Freije, 2002; Zavala et al., 2008).

The early uplift of the different topographic elements of the area (Cordón de la Piedra Santa, Sierra de Chacaico, Picún Leufú anticline, and associated features) falls within a regional event of intraplate deformation which started in Early Jurassic times, and which is well documented along the subsurface trace of the Huincul deformational zone (Grimaldi and Dorobek, 2011; Mosquera and Ramos, 2006; Pángaro et al., 2009; Silvestro and Zubiri, 2008; Vergani et al., 1995; Zavala and Freije, 2002Zavala et al., 2008). This extensive deformation process was the result of the conjunction between an east–west oriented basement weakness zone, and a NNW to NW oriented stress field (Mosquera and Ramos, 2006; Mosquera et al., 2011; Rosenau, 2004; Silvestro and Zubiri, 2008; Vergani, 2005).

4. Provenance data

Sedimentary provenance and U–Pb ages of detrital zircons were analyzed in rocks from the Tordillo and Quebrada del Sapo Formations (Fig. 2). The main objective was to define the relation between

exhumed areas and possible sedimentary sources in Late Jurassic times. On this basis, the timing of uplift of Huincul High is evaluated.

4.1. Petrography and provenance

The study rocks are conglomerates from the Tordillo (Groeber, 1946) and Quebrada del Sapo (Leanza, 1993; Parker, 1965) Formations that crop out in the area of influence of the Huincul High (Fig. 1). Sample TOR-07 is a fine-grained conglomerate from the Tordillo Formation at the Arroyo Covunco locality (38°47′40.55″S–70°11′42.41″W) (Fig. 7a and b); sample TOR-09 is a conglomerate from the base of the Quebrada del Sapo Formation at Arroyo Picún Leufú (39°12′47.91″S–70°03′55.13″W), and sample TOR-10 corresponds to a coarse conglomerate of the same unit but cropping out in the Fortin 1° de Mayo area (39°25′32.50″S–70°39′9.10″W) (Fig. 7c, d, e and f). Petrographic classification (Folk et al., 1970) of the matrix of conglomerates corresponds to feldspathic litharenite (samples TOR-07 and TOR-09) and to litharenite (sample TOR-10).

In sample TOR-10, polycrystalline quartz is the most common type among the quartz grains. Monocrystalline quartz with straight extinction predominates over grains with undulatory extinction. The limpid monocrystalline quartz grains with straight extinction and the presence of embayment with preservation of the volcanic matrix suggest a high temperature volcanic origin. The presence of some crystals with intergrowth textures supports plutonic sources. The polycrystalline quartz with elongate shape and subparallel orientation were

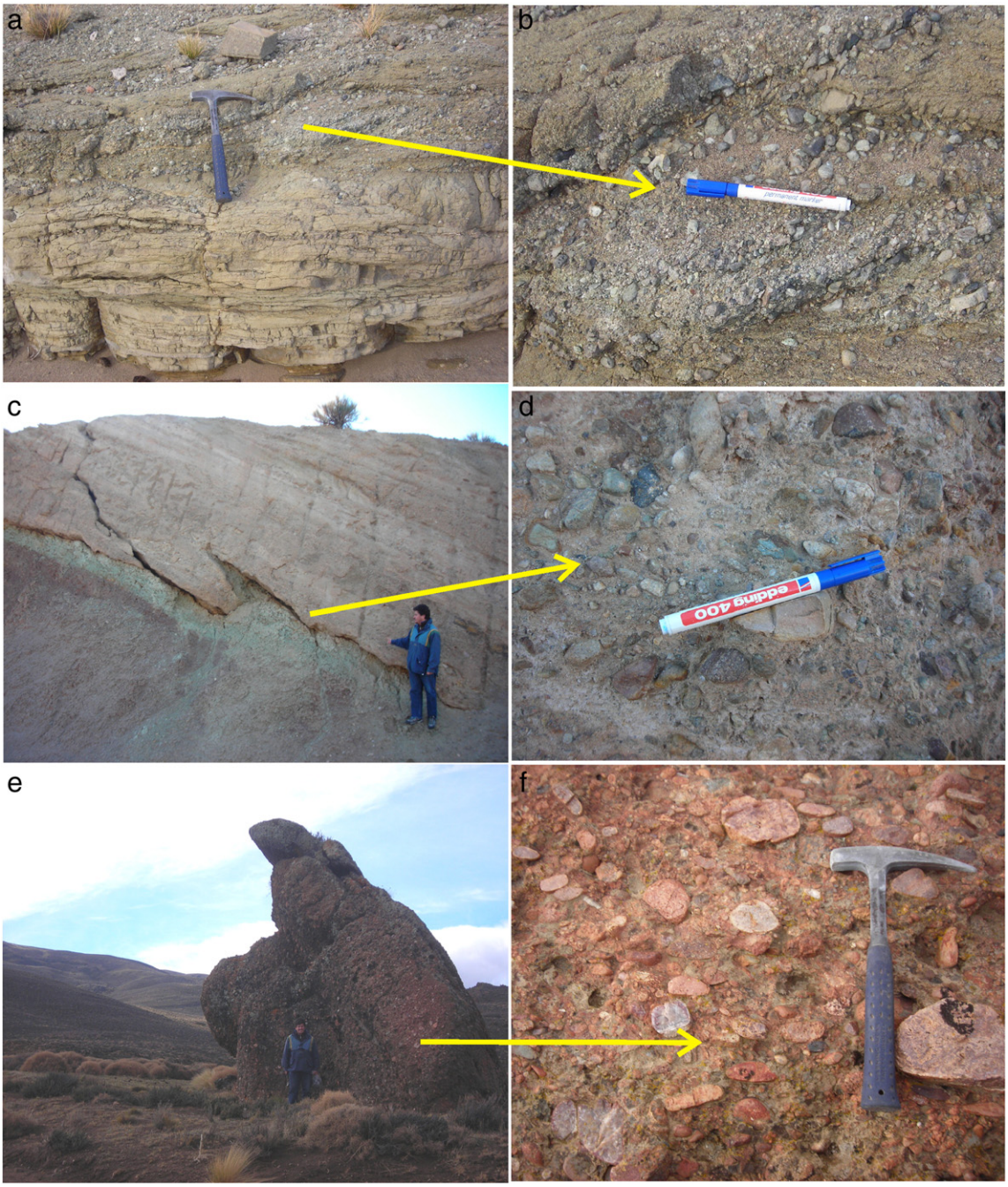

Fig. 7. Photographs of outcrops of the U–Pb samples localities; a–b) fine-grained conglomerate and sandstone levels from the Tordillo Formation at the Arroyo Covunco locality (sample TOR-07); c–d) conglomerate from the base of the Quebrada del Sapo Formation at Arroyo Picún Leufú, with a detail of the base of this strata (sample TOR-09); e–f) a coarse conglomerate of the Quebrada del Sapo Formation cropping out in the Fortin 1° de Mayo area, see the rounded granite and acid volcanic clasts in the detail (sample TOR-10).

most likely derived from a metamorphic source (Blatt, 1967; Ghazi and Mountney, 2011). The detrital quartz grains of this sample were probably derived from the erosion of several source rocks: volcanic, plutonic, and metamorphic. The ratio of plagioclase to total feldspar is 0.62; this value is expected for sediments derived from volcanic terranes (Dickinson 1970; Dickinson and Rich 1972; Ingersoll, 1979). Both alkali feldspar and plagioclase are slightly altered by silt and are occasionally replaced by carbonate. There are abundant rock fragments (61%), the most common being volcanic with seriate and granular textures; also volcanic rock fragments with lathwork, microlitic and vitric textures were identified (Fig. 8b). This clearly suggests provenance from a volcanic arc. The presence of metamorphic rock fragments is notable, mainly gneiss and low grade schists. The presence of minor amounts of sedimentary rock fragments, including siltstones and sandstones suggests additional sedimentary provenance.

Detrital quartz grains in the sample TOR-09 are abundant, the most common being the monocrystalline type. Among the monocrystalline type the grains with straight extinction are the most abundant (Fig. 8c). The quartz grains are limpid, with inclusions and embayments. In a similar way to sample TOR-10, the origin of this monocrystalline quartz may be volcanic or plutonic. The proportion of polycrystalline quartz drops drastically and is related to a metamorphic source. The ratio between plagioclase and total feldspar is 0.3, a value far from the 0.75 used as a limit for the volcanic derived sands, and therefore a mixed source is probable. Rock fragments also provide information on the source of this sample. The most common lithic fragments are the volcanics but in a much lower proportion than in sample TOR-10 (Fig. 8c). The main composition of this volcanic rock fragments are felsic. It is also notable the presence of small but significant amounts of plutonic rock fragments suggesting a nearby source of this type. The presence of minor amount of sedimentary rock fragments, mainly siltstones suggests an additional sedimentary source rock.

The detrital quartz grains in the sample TOR-07 are abundant but less abundant than in samples TOR-9 and TOR-10. In a similar way to sample TOR-09, the monocrystalline type is the most common (Fig. 8d). Among the monocrystalline type the grains with straight extinction are the most abundant. The quartz grains are limpid, with inclusions and embayments (Fig. 8d). Just as in the interpretation of the previous samples, the origin of this monocrystalline quartz may be volcanic or plutonic. Several grains with embayment and volcanic matrix support a volcanic origin. A direct relation between metamorphic rock fragments and the occurrence of polycrystalline quartz is once more recognized. The ratio between plagioclase and total feldspar is 0.5 suggesting a mixture of sources. The composition in a broad sense is very similar to sample TOR-9, but the proportion of volcanic, metamorphic and plutonic fragments is smaller in comparison with the sedimentary fragments. This sample is located further east of the volcanic arc and the metamorphic terranes and it is further north of the volcanic and plutonic sources of the Huincul High. The dominant lithic fragments are of volcanic rocks but in a lower proportion than in samples TOR-10 and TOR-09. The most common are felsic, but the proportion of mafic rocks is notably higher. This increment of the sedimentary fragments indicates exposure of previous Mesozoic units.

Overall, the characteristic clast populations in the three studied samples indicate a provenance consistent with an active volcanic arc together with uplifted metamorphic and plutonic terranes. Some volcanic rock fragments that constitute the pseudomatrix indicate a rapid deformation of the rock. The feldspathic litharenites (TOR-97

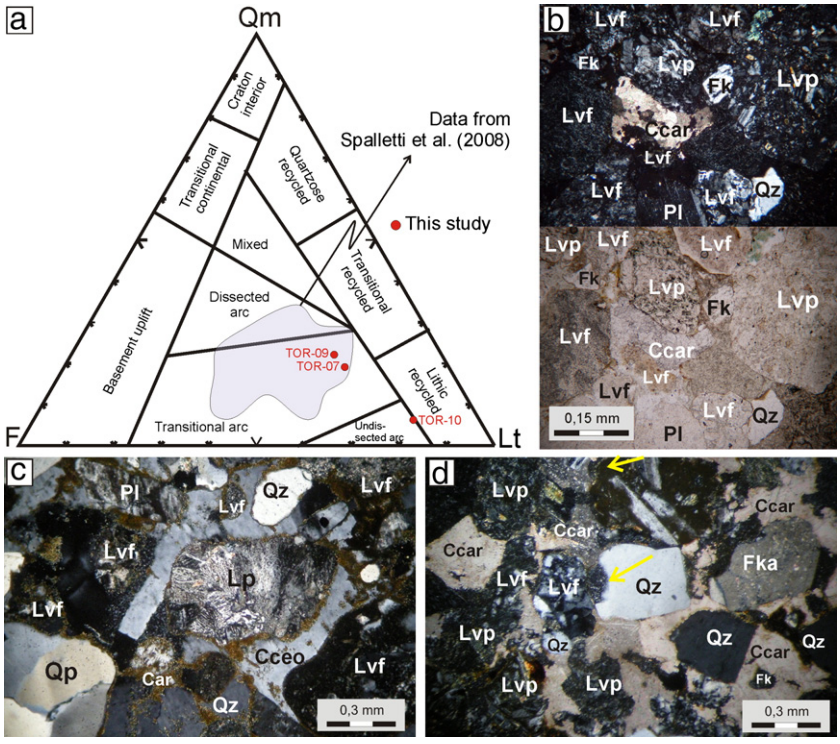

Fig. 8. a) Qm-F-Lt Dickinson et al. (1983) tectonic setting plot that shows detrital data from this study and from Spalletti et al. (2008; 52 sandstones in shaded area). Qm: monocrystalline quartz grains; F: feldspar grains; Lt: lithic grains including polycrystalline quartz. b), c), and d) Microphotographs of thin section from the U–Pb samples and its diagnostic detrital grains and cements. All photos with crossed nicols except the lower b. b) Sample TOR-10; lithoarenite showing the abundance of volcanic lithic fragments both felsitic (Lvf) and mafic (Lvp). Scarce grains of monocrystalline quartz (Qz), feldspar (Fk) and plagioclase (Pl) are also shown. The cement is carbonate probably calcite (Ccar). c) Sample TOR-09; a plutonic rock fragment (Lp) with intergrowth textures reveals a plutonic source nearby. Monocrystalline (Qz) and polycrystalline (Qp) quartz grains were identified as well as volcanic lithic fragments, mainly felsitic (Lvf) with seriate and granular textures and plagioclase grains (Pl). The cements are zeolitic (Cceo) probably laumontite and clay rims (Car). d) Sample TOR-07; the volcanic origin of the monocrystalline quartz (Qz) grains can be supported by the presence of the embayment with the volcanic groundmass preservation (yellow arrows). In this view of the sample can be noticed the higher proportion of mafic volcanic rock fragments (Lvp) over the felsic ones (Lvf). Some feldspar grains were altered to calcite (Fka). The common cement is carbonate (Ccar) with thin clay rims.

Table 1
Summary of the morphological features and internal structures of the main zircon populations described in the studied samples (TOR-7, TOR-09, and TOR-10) of the Tordillo Formation.

Populations	Form	Habit	Color	Elongation	Internal structure
Population I **(P1)**	Subrounded to subidiomorphic	Prismatic, pyramidal crystal, (< acicular zircons)	Yellow, transparent	3 to 5 (>5)	Inclusions, oscillatory zoning
Population II **(P2)**	Idiomorphic	Multifaceted crystal	Pink	<2	Faint zoning (oscillatory zoning)
Population III **(P3)**	Rounded		Yellow, pink, transparent	<2	Inclusions, faint zoning (oscillatory zoning)

and TOR-09) plot in the transitional arc field and the litharenite (TOR-10) plots in the undissected arc field of Dickinson et al. (1983) diagram (Fig. 8a). This evidence clearly indicates that volcanic rocks may have been the major source. This conclusion coincides with provenance analyses of Spalletti et al. (2008) (see Fig. 8a).

4.2. Detrital zircons results

Heavy mineral studies, especially of detrital zircon, are a widely used tool in the analysis of the provenance of sedimentary basins (Morton and Hallsworth, 1999). Many analyses of sedimentary provenance have demonstrated the utilities of the study of the external and internal properties of zircons, and even more so when it is combined with U–Pb geochronology data as well as with CL or BSE images (Bahlburg et al., 2009; Fedo et al., 2003; Goodge et al., 2004; Mueller et al., 1994). One of the main objectives of this study is to describe the morphology and internal structure of the detrital zircons in order to define the most representative populations. Subsequently, the patterns and main peaks of U–Pb ages were identified as well as the maximum depositional stratigraphic ages in order to interpret the possible sediment sources.

4.2.1. Analysis of morphology and internal structures in the zircons

Detrital zircons separated from the samples (TOR-07, TOR-09, and TOR-10) can be grouped into three main populations according to their shape, color, habit, size, and elongation (Table 1). In sample TOR-07 the most abundant population (P1) comprises short (~100 μm) and long (>250 μm) zircon grains with prismatic habit, subrounded to subidiomorphic forms, and yellow color. Many grains have inclusions and fractures. The second largest population (P2) is characterized by idiomorphic pink multifaceted crystals. Population P3 is the least abundant, formed by rounded zircons with evidence of several cycles of sedimentation (Fig. 9a). In the SEM images zircon grains display typically magmatic textures characterized by oscillatory zoning. There were also many prismatic zircons with high aspect ratio (elongation ~5:1), oscillatory zoning, and inclusions that indicate a possible volcanic origin (Fig. 9b).

Two main zircon populations were recognized in sample TOR-09 according to external properties. Population P1 is characterized by prismatic zircons in varied sizes, between 100 and 450 μm in length; elongation varies between 3 and 5. They are mostly transparent or yellow in color, with inclusions, subrounded to subidiomorphic, and some of them present bi-pyramidal crystal forms. Population P2 included idiomorphic, multifaceted pink zircons. Another less abundant population (P3) with rounded grains (Fig. 9c) is also observed. The SEM images show crystals principally with internal textures characterized by oscillatory zoning indicating a magmatic origin (Fig. 9d).

Detrital zircons from sample TOR-10 are characterized by a predominance of a population (P1) where the crystals have short and long prismatic habit. Acicular zircons were also observed. The forms were subrounded to subidiomorphic; there were also crystals with bi-pyramidal form. They are mostly transparent or yellow in color, inclusions and fractures are present. There is a smaller population (P2)

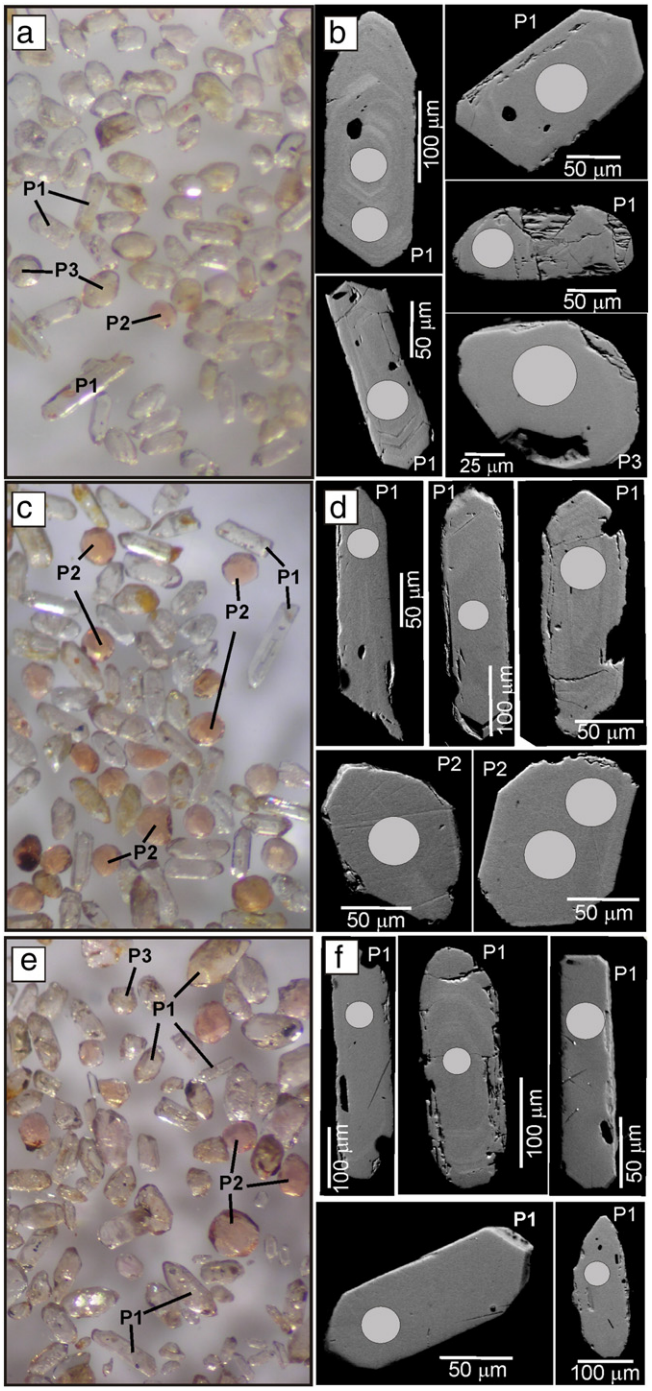

Fig. 9. Binocular and backscattering electrons images from the studies samples, a–b) TOR-07, c–d) TOR-09, and e–f) TOR-10. P1, P2, and P3 zircons populations defined in the text.

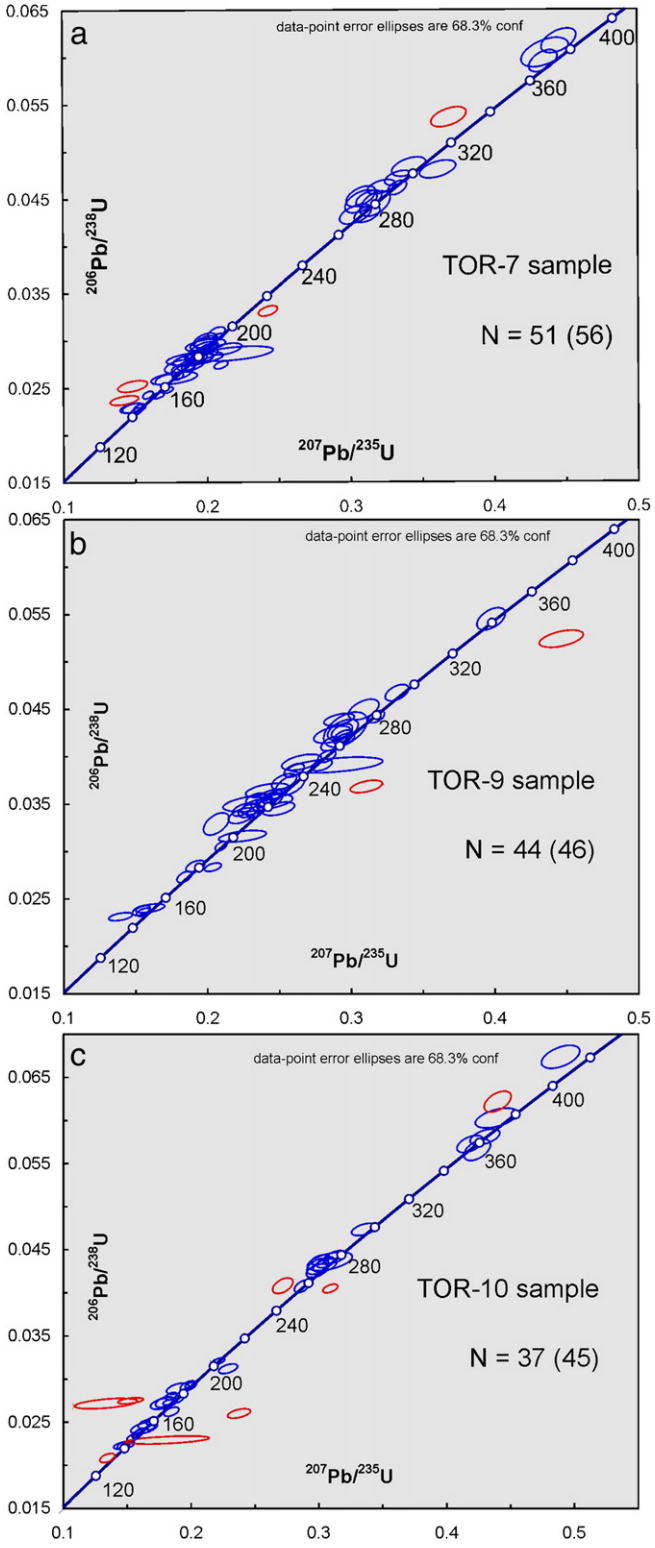

Fig. 10. Concordia plots from the U/Pb samples analyzed, a) TOR-07, b) TOR-09, and c) TOR-10. The detrital zircon ages showed in the concordia plots are the concordant ages (in blue) and discordance ages (in red) discussing in the text. One discordant age falls outside of the TOR-07 diagram (a).

that is represented by pink zircons with idiomorphic forms, multifaceted crystals (Fig. 9e). The SEM images show faint internal structures and the oscillatory zoning is difficult to recognize. This can only be observed in a few grains with prismatic long habit and pyramidal forms that may indicate a volcanic origin (Fig. 9f).

4.2.2. U–Pb age peaks

Detrital zircons from samples described above were randomly separated and dated by U–Pb LAM–MC–ICP–MS (the Supplementary Material includes a description of analytical methods and a complete listing of analytical data). The maximum age peaks obtained were analyzed with respect to populations P1, P2, and P3 previously defined through the morphological analysis and internal structures.

A total of 55 zircon grains from sample TOR-07 were mounted and dated. We obtained 56 ages but results from 5 analyses were rejected due to high discordance (Fig. 10a). The spectra of concordant ages are characterized by two main peaks: the maximum at ca. 178 Ma (50%) and a secondary at ca. 283 Ma (20%). Smaller groups of ages appear at ca. 143–158 Ma (12%) and between ca. 372 and 386 Ma (5%). Two Precambrian grains (ca. 848 and 1524 Ma) are present (Fig. 11a); although discordant, these ages it are significant and it is clear that they are much older than the rest of the populations. The grains with younger ages (ca. 178 Ma) are typically represented by zircons from the P1 population. The zircons with ages at ca. 283 Ma are also included

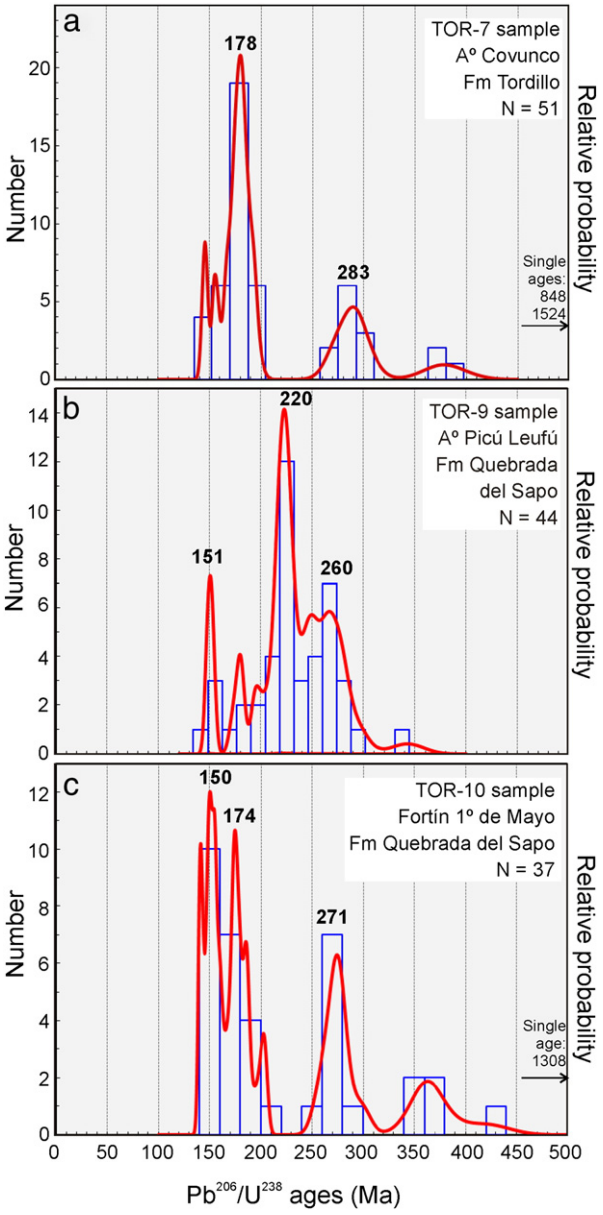

Fig. 11. Frequency histogram and relative probability plots of Pb^{206}/U^{238} ages on detrital zircons from Tordillo and Quebrada del Sapo samples.

in P1 but the crystals are moderately more rounded (Fig. 9a and b). The older ages (between 372 and 386 Ma) correspond to the P3 population.

In sample TOR-09, 44 crystal grains were analyzed and we obtained 46 ages (including core and overgrowth). Results from 2 grains were rejected due to high discordance (Fig. 10b). The age pattern is characterized by three main peaks: ca. 151 (9%), 220 (45%), and 260 Ma (36%). A smaller group is present between 173 and 180 Ma (7%) and there is an isolated age at ca. 342 Ma (Fig. 11b). The main peak at ca. 220 Ma is formed by zircon grains that are included in the P2 population; in this group there are also subordinate crystals from the P1 population, while zircon peaks at ca. 151 and 260 Ma are only represented by grains from the P1 population (Fig. 9c and d).

The number of ages obtained in sample TOR-10 was 45 and 2 results with high uncertainties were rejected; another 6 data showed highly discordant ages and were also rejected (Fig. 10c). The 37 remaining ages are distributed between three main peaks: ca. 150 Ma (30%), 174 Ma (24%), and 271 Ma (24%). Smaller peaks appear at ca. 201 Ma (5%) and 356 Ma (11%). Single zircons give ages at ca. 420 Ma (Late Silurian) and 1308 Ma (Mesoproterozoic) (Fig. 11c). The zircon peaks with ages at ca. 150, 174, and 260 Ma match those described in the P1 population. In particular, those zircons with large prismatic and acicular habits with a little evidence of transport have the younger ages (~150 Ma); this suggests a volcanic origin probably coeval with the sedimentation.

4.2.3. Maximum depositional age

The age of the Tordillo and Quebrada del Sapo Formations is classically assigned to the Kimmeridgian, although in the southern part of the basin some authors extended the age to early Tithonian (Cucchi et al., 2005; Leanza and Hugo, 1997) based on their stratigraphic position. The minimum age of these units is defined by the concordant deposition of the overlying Vaca Muerta Formation. The age of the base of the Vaca Muerta Formation is assigned to the late early Tithonian based on its abundant ammonoid fauna (Leanza, 1981; Riccardi, 2008a,b). The peaks of youngest U–Pb ages that are statistically significant obtained in our analysis were: ca. 178 Ma (Toarcian) in sample TOR-07; ca. 151 Ma (Kimmeridgian–Tithonian boundary) in sample TOR-09, and ca. 150 Ma (early Tithonian) for sample TOR-10 (see Fig. 9). Also, the U–Pb age distribution of all detrital zircons analyzed (N = 132; three samples) shows a clear peak at 153 Ma (Fig. 12). Possibly, this last age is a better value to represent the maximum depositional age of the sequence. However, it is noteworthy that in all the samples analyzed a significant number of ages, ca. 145 Ma, are younger than the currently accepted Kimmeridgian/Tithonian boundary. That is to say, these detrital zircon ages are not in agreement with the absolute ages for the Kimmeridgian (155.7–150.8 Ma) and the Tithonian (150.8–145.5 Ma) published in the Geological Time Scale for the Jurassic (Ogg, 2004). These younger zircon ages are concordant and they have small analytical errors, but they are difficult to explain. The meanings of those ages are beyond the scope of this work.

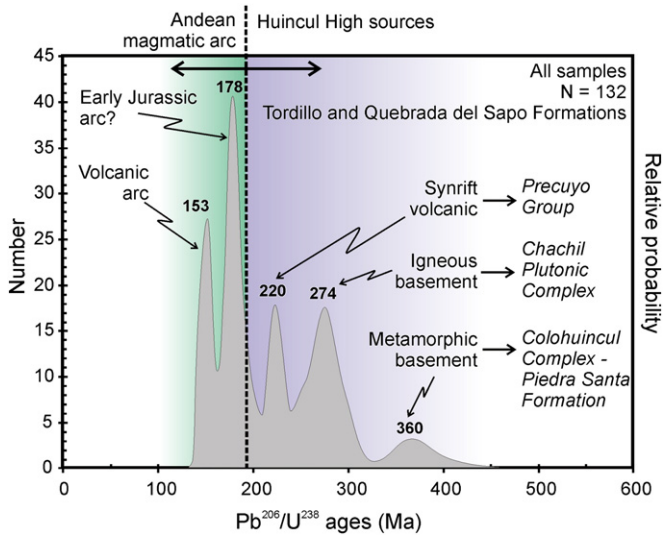

Fig. 12. Summary of the U/Pb zircon ages for all three analyzed samples (TOR-07, TOR-09, and TOR-10). Within the main peaks of ages, the possible source areas are interpreted.

5. Discussion

5.1. Source regions

Several provenance studies have suggested that there were two main sources for the original sediments of the Tordillo Formation and equivalent successions: the Andean magmatic arc to the west and the Huincul High within the Neuquén Basin (Gulisano, 1988; Spalletti and Colombo, 2005; Spalletti et al., 2008). However, until the present study there was neither evidence in the Tordillo Formation about the absolute ages of the source areas at the moment of their deposition, nor of the relative importance that these areas had through the basin. Moreover, the role of the early deformational stages in the generation of relief was not known, and consequently their importance in the Jurassic configuration of the southwestern Neuquén Basin cannot be assessed.

Paleocurrent analyses in the Tordillo Formation on both sides of the Huincul High are consistent with both potential western and southern source regions. Analyses from outcrops on the western side indicate axial systems, parallel to the Andean chain, with N to NE trends (Gulisano, 1988; Spalletti and Colombo, 2005). In the northern outcrops there are also paleocurrents indicating transport to the E, which suggest a provenance from the west due to a positive area probably linked to the Andean magmatic arc (Spalletti and Colombo, 2005). In the southern Picún Leufú depocenter the paleocurrents at the base of Quebrada del Sapo Formation show a SW trend (Zavala et al., 2005). This direction is consistent with emerged areas along the western Huincul High, where structural features linked to this morphotectonic unit shows evidence of early growth between the Early and the Late Jurassic.

Petrological and geochemical analyses on conglomerates and sandstones from the Tordillo Formation were made by Spalletti et al. (2008) north of the Huincul High. They indicate volcanic rocks as the main source of the sediments during deposition of the Tordillo Formation. Its composition varies from acidic in the south and west to mafic in the northern Neuquén basin (Spalletti and Colombo, 2005; Spalletti et al., 2008). This bimodal composition allowed the authors to suggest that part of the detrital material in the Tordillo Formation was derived from bimodal volcanic successions developed in a synrift environment (Franzese and Spalletti, 2001; Spalletti et al., 2008). However, there were still no radiometric ages of detrital material to confirm the absolute ages of the sedimentary source areas in the Tordillo Formation. Consequently, the detrital zircon ages obtained here allow us to define for the first time the absolute ages, compositions, and relative importance of the source areas from the studied units (Fig. 12).

In sample TOR-07 the sedimentary provenance is clearly from Jurassic sources (62%) with a main peak at ~178 Ma (Toarcian). The external morphologies and internal textures of the zircons indicate a magmatic origin that is probably volcanic. The zircons morphology and the petrographic features of this sample are coherent with volcanic and plutonic sources. Jurassic plutonic rocks with similar ages (~173 Ma; Castro et al., 2011) are widely developed in the North Patagonian Batholith as part of the Andean magmatic arc). Thus, we interpret that the main source of sediment supply for this sample was the Andean arc, located along the western margin of the basin (Fig. 1). Nevertheless, according to the paleocurrent

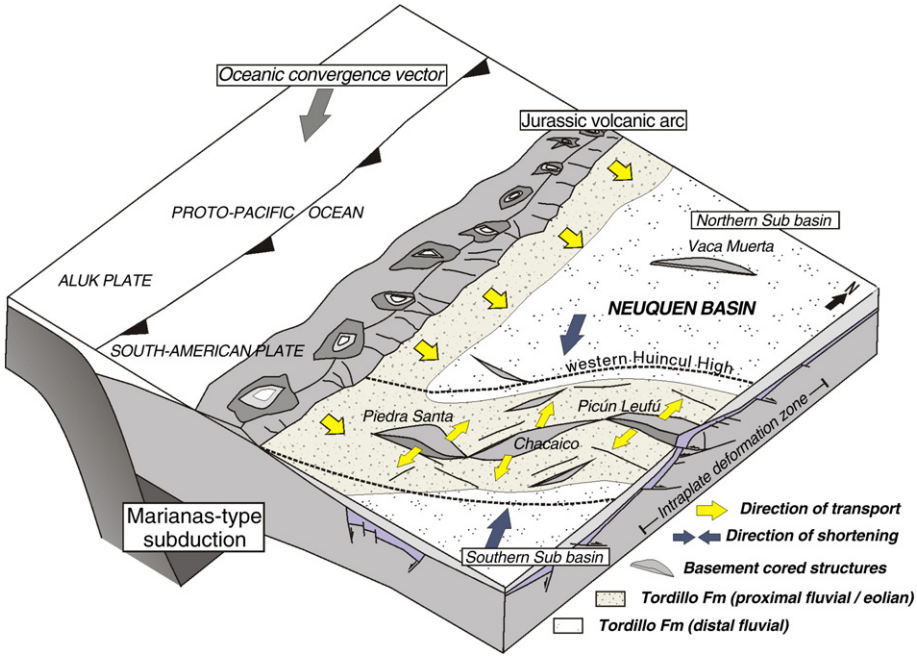

Fig. 13. Late Jurassic paleogeography and geological setting of the Neuquén Basin. Note the potential source areas for the basin: presence of a western magmatic arch and emerged areas along the east–west oriented Huincul deformational zone.

measurements and the fragments of sedimentary rocks observed, it is possible that the detrital zircons with ages of ~178 Ma were derived from the reworking of previous units (e.g. pre-Cuyo and/or Cuyo groups), which crop out along the entire axis of the Huincul High. Here they constitute the core and the limbs of the early uplifted structural features (Cordón de la Piedra Santa, Sierra de Chacaico, Picún Leufú anticline, and associated structural features) (Figs. 3 to 6). According to Ploszkiewicz et al. (1984), about 2000 meters of the Choiyoi, Pre-Cuyo Group, and Cuyo Group sedimentary rocks were partially eroded in the axial part of the Huincul High.

A minor peak (5%) is seen at ~283 Ma (Early Permian). Similar U–Pb zircon ages were found by Schiuma and Llambías (2008) in drill cores in neighboring areas of the Huincul High (ca. 286–284 Ma). These authors correlate the Early Permian plutonic rocks to the base of Choiyoi Group (Llambías et al., 1993). Therefore, these basement rocks could be the source of the Permian detrital zircons in the sample TOR-07. The Late Devonian isolated ages could also be related with rocks from the Huincul High; more precisely from the igneous-metamorphic rocks (e.g. Colohuincul Complex and/or Piedra Santa Formation) linked to the early uplifted basement cored structures which conform the main topographic features along the exposed portion of the Huincul High (Cordón de la Piedra Santa, Sierra de Chacaico, and associated features).

Sample TOR-9 also has a significant amount of Jurassic zircons (~151 and 178 Ma) of magmatic origin and possibly volcanic, but this group does not constitute the most important population (19%). Similar ages were also found by Castro et al. (2011) in the North Patagonian Batholith. This Kimmeridgian peak reflects a sediment supply from the Andean arc that was probably contemporaneous with sedimentation. The most important peak of relative frequency is ~220 Ma (44%), in which the zircons are mostly idiomorphic and have a magmatic origin. The base of pre-Cuyo Group is composed of a thick sequence of volcanic and volcaniclastic rocks with ages between ca. 219 and 182 Ma (Franzese et al., 2006; Pángaro et al., 2002; Rapela et al., 1983; Schiuma and Llambías, 2008). These rocks are widely distributed along the Huincul High, where they form the core of several topographic features that were partially uplifted by the time of the deposition of the Tordillo Formation (Figs. 3 and 4). These outcrops are the best candidates to be the source of the Late Triassic zircons that are present in sample TOR-9. It is important to note that there are also magmatic rocks dated between ~225 and 205 Ma that are widely exposed southeast of the Neuquén Basin in the Central Patagonian Batholith (Cingolani et al., 1991; Rapela et al., 1991, 2005). However, paleocurrent measurements in the Picún Leufú depocenter indicate an orientation of drainage from the northeast, discarding the southeastern Central Patagonian Batholith as a possible source. The third and last component at ~260 Ma (37%) indicates a contribution from the Permian granitoids of Chachil Plutonic Complex (Leanza, 1990), which constitute the core of large anticlines that form the principal topographic elements in the exposed portion of the Huincul High (Cerro Granito, Sierra de Chacaico, and Cordón de la Piedra Santa) (Fig. 3). In sample TOR-09 it is evident that the provenance is mainly from outcrops linked to the south and northwest-verging structures which integrate the Huincul deformation zone, and to a lesser degree from the western volcanic arc.

Finally, sample TOR-10 shows a maximum frequency of ages at ca. 150 Ma (Early Tithonian), this peak is the youngest from the three samples. Zircons have morphologies and internal textures that indicate a volcanic origin with little evidence of long transport. This is consistent with its relative westernmost position, next to the Andean arc (Fig. 1). Therefore, these zircons reflect a supply from this region and indicate that there is a contemporaneous active Late Jurassic arc. Moreover, due to the low level of transport observed in the zircons, it is probable that they were deposited through ash-fall tuffs or cineritic layers. This evidence is clearly in agreement with petrographic results which indicate an undissected arc source (Fig. 8a). In addition, Early to Middle Jurassic zircons (peak at ~174 Ma) were also observed in this sample, which are comparable with ages from the North Patagonian Batholith. The secondary peaks (~271 and 356 Ma) indicate that there are basement sources, such as the Chachil Plutonic Complex and the Late Paleozoic igneous-metamorphic rocks (Colohuincul Complex and Piedra Santa Formation). This pattern of zircon ages suggests that the detrital material came mainly from the Andean magmatic arc and to a lesser extent from the already partially uplifted Huincul High (Sierra de Chacaico, Cordón de la Piedra Santa, Picún Leufú anticline, and adjacent areas).

5.2. Tectonic implications

The Andean subduction cycle started in the Southern Central Andes in the Early Jurassic. During that time, South America was moving as part of West Gondwana to the northeast. This absolute plate motion implied a negative trench roll-back with generalized extension. In this context, a Jurassic magmatic arc developed in an attenuated crust (Ramos, 2010). This situation lasted until the Late Cretaceous, when the change from thermal retroarc subsidence to a foreland basin subsidence in the Neuquén Basin took place, due to a compressional regime which started in most of the Andes during that time, and resulted in the uplift of the Andean chain at these latitudes (Cobbold and Rossello, 2003; García Morabito and Ramos, 2011a; Ramos, 2010; Tunik et al., 2010; Vergani et al., 1995; Zamora Valcarce et al., 2006). This orogenic episode coincides with the beginning of the absolute motion of South America to the west due to the Western Gondwana break-up (Ramos, 2010). Prior to the Late Albian and the Early Cenomanian, no significant contractional deformation is reported in the Central Andes.

The paleogeography of the study area indicates the existence of Late Jurassic emerged areas developed within a generalized regional subsidising context as a consequence of localized pre-Andean deformation. They define an uplifted positive element, which represents an anomaly in the context of the Jurassic regional configuration of the South American margin, characterized by subsidence and generalized extension.

There are several parameters which might have played a key role in the inception of Jurassic deformation and the development of an extensive east–west oriented corridor of deformation where emerged areas concentrated. Weakness zones in the continental crust inherited from old sutures among terranes, or from previous extensional basement faults, commonly exert an important control in localizing subsequent deformation (Ramos, 2010; Vietor and Echtler, 2006). The Huincul High is related to a major crustal weakness zone, which concentrated the rifting during early Mesozoic times, and subsequent deformation in the Andean cycle. This continental weakness zone was recently interpreted as linked with the suture developed during the amalgamation of Patagonia to the rest of Gondwana in late Paleozoic times (Mosquera et al., 2011; Ramos, 2008).

According to several plate reconstructions, the slip vector between the different oceanic plates and South America experienced significant anticlockwise rotations between the Early Jurassic and the Early Cretaceous. By the time of the inception of deformation along the Huincul High, the oceanic convergence vector had a north–northwest orientation (Jaillard et al., 1990; Mosquera and Ramos, 2006; Ramos, 2010; Scheuber et al., 1994; Zonenshayn et al., 1984).

Detailed structural studies carried out in the area of influence of the Huincul High on both sides of the Andean chain, determined NNW to NW oriented shortening axes acting during Jurassic and Early Cretaceous times (Mosquera, 2008; Repol, 2006; Rosenau, 2004; Silvestro and Zubiri, 2008; Vergani, 2005). This orientation implies no significant refraction of the strain axis relative to the plate motion direction, as expected in highly obliquely convergent margins where deformation is commonly partitioned into strike-slips and contractional deformation (Teyssier et al., 1995; Tikoff and Teyssier, 1994). Partitioning commonly increases the misfit between the plate motion and the contraction direction.

When partition is low or incomplete only one part of the strike-slip component is taken up by discrete strike-slip faulting. In this case deformation is distributed homogeneously along wide transpressional crustal belts of high structural complexity. In such systems, large crustal portions will deform in a mixed way due to the accommodation of orthogonal and a lateral shear components, resulting in a wide range of styles of deformation (Teyssier et al., 1995; Tikoff and Teyssier, 1994). The Huincul High, which defines an east–west striking diffuse zone, accommodated displacement trough a combination of NE-trending thrust faults, east–west oriented transpressional structures with significant slip components, and minor transtensional and transpressional reactivations of NW to NNW previous normal faults.

The favorable disposition of this east–west oriented basement weakness zone respect the estimated directions of shortening transmitted to the foreland due to a NNW orientation of the convergence vector, probably resulted in an effective mechanism in accommodating deformation along this margin orthogonal disposed feature. Intraplate strain was probably controlled by the conjunction of these parameters (orientation of the slip vector and east–west oriented continental weakness zone), resulting in a wide transpressive crustal deformational belt which extended for hundreds of kilometers to the foreland (Mosquera and Ramos, 2006), in the context of a subsiding basin developed in a margin dominated by generalized extension. This complex deformational process exerted a notable influence in the configuration and paleogeography of the Neuquén Basin as evidenced by the obtained zircon ages patterns, truncating the entire basin due to emerged areas which concentrated along this corridor of deformation.

The tectonic scenario in which this intraplate deformation took place, represent a variant of the classical models described by Ziegler et al. (1998), who only defined these processes within collisional or Andean-type orogens exclusively dominated by compression. Considering the scenario in which the Huincul System developed and the characteristics of this deformational zone, a special type of intraplate deformation can be interpreted as occurred in Jurassic times in the Central Andes during the beginning of the Andean cycle (Fig. 13).

6. Concluding remarks

1) A stratigraphic and structural record for a pulsed contractional deformation which occurred between Early and Late Jurassic times is derived from field surveys carried out along the exposed portion of the Huincul High. It is documented through multiple unconformities and growth geometries linked to NE and east–west oriented growth structures extensively developed across the region.
2) The pattern of zircon ages from the analyzed Late Jurassic successions indicates that they have a clear provenance from sources located within the southern Neuquén basin along the Huincul deformation zone. The data confirm the presence of emerged elements as source areas that divided the Neuquén basin in two sectors at least during the Kimmeridgian. The Tordillo Formation outcrops north of the Huincul High have a dominant provenance from the Andean Jurassic arc; while the Quebrada del Sapo Formation, south of the Huincul High, has a significant supply from Late Triassic (220–200 Ma) and Late Permian (280–260 Ma) sources, indicating a provenance from the Precuyano Group and Chachil Plutonic Complex in the axial exposures of the Huincul zone. Integration of data documents the importance of the early deformational events as a first-order control in the Late Jurassic configuration and paleography of the Neuquén Basin.
3) Field data and provenance characteristics of detrital zircons, confirm the presence of an ancient positive element within the southern Neuquén Basin. Its genesis falls within the early history of the Huincul deformation zone, where several structural features indicate pulses of growth since Early Jurassic times prior to the main Andean contractional cycle started in the Late Cretaceous (Tunik et al., 2010). Therefore, these data document for the first time the importance of the early contractional phases in the relief construction in the southern Central Andes, reinforcing previous hypotheses about pre-Andean intraplate deformation concentrated along this extensive east–west oriented basement weakness zone.

Acknowledgements

Maximiliano Naipauer acknowledges the financial support received by CONICET, Bunge & Born Foundation, and ANPCyT PICT-2010-2099, Argentina. Marcio Pimentel acknowledges continuous financial support from CNPq. We want to thank the reviewer's comments that helped to improve the quality of the paper and the Editor of the Journal Fabrizio Storti. This is the contribution R-54 of the Instituto de Estudios Andinos “Don Pablo Groeber” (CONICET-UBA).

Appendix A. Supplementary data

Supplementary data to this article can be found online at doi:10.1016/j.tecto.2011.12.017.

References

Bahlburg, H., Vervoort, J.D., Du Frane, S.A., Bock, B., Augustsson, C., Reimann, C., 2009. Timing of crust formation and recycling in accretionary orogens: insights learned from the western margin of South America. Earth-Science Reviews 97, 215–241.

Blatt, H., 1967. Original characteristics of quartz grains. Journal of Sedimentary Petrology 37, 401–424.

Castro, A., Moreno-Ventas, I., Fernández, C., Vujovich, G., Gallastegui, G., Heredia, N., Martino, R.D., Becchio, R., Corretgé, L.G., Díaz-Alvarado, J., Such, P., García-Arias, M., Liu, D.Y., 2011. Petrology and SHRIMP U/Pb zircon geochronology of Cordilleran granitoids of the Bariloche area, Argentina. Journal of South American Earth Sciences. doi:10.1016/j.jsames.2011.03.011.

Chernicoff, C.J., Zappettini, E.O., 2004. Geophysical evidence for terrane boundaries in south-central Argentina. Gondwana Research 7, 1105–1116.

Chotin, P., 1976. Essai dinterprétation du Bassin Andin chiléno-argentin mésozoique en tant que bassin marginal. Annales de la Société Géologique du Nord, Lille 96 (3), 177–184.

Cingolani, C., Dalla Salda, L., Hervé, F., Munizaga, F., Pankhurst, R.J., Parada, M.A., Rapela, C.W., 1991. The magmatic evolution of northern Patagonia; new impressions of pre-Andean and Andean tectonics. In: Harmon, R.S., Rapela, C.W. (Eds.), Andean magmatism and its tectonic setting: Boulder, Colorado: Geological Society of America Special Paper 265, pp. 29–44.

Cobbold, P.R., Rossello, E.A., 2003. Aptian to recent compressional deformation, foothills of the Neuquén Basin, Argentina. Marine and Petroleum Geology 20, 429–443.

Cucchi, R., Leanza, H.A., Repol, D., Escosteguy, L., González, R., Daniela, J.C., 2005. Hoja Geológica 3972-IV, Junín de los Andes. Provincia del Neuquén. Instituto de Geología y Recursos Minerales, Servicio Geológico Minero Argentino, Boletín 357 102 pp., Buenos Aires.

de Ferraríis, C.I.C., 1947. Edad del arco o dorsal antigua de Neuquén oriental de acuerdo con la estratigrafía de la zona inmediata. Revista de la Asociación Geológica Argentina 2 (3), 256–283.

Dickinson, W.R., 1970. Interpreting detrital modes of graywacke and arkose. Journal of Sedimentary Petrology 40, 695–707.

Dickinson, W.R., Rich, E.I., 1972. Petrologic intervals and petrofacies in the Great Valley Sequence, Sacramento Valley, California. Geological Society of American Bulletin 83, 3007–3024.

Dickinson, W.R., Beard, L.S., Brakenridge, G.R., Erjavec, J.L., Ferguson, R.C., Inman, K.F., Knepp, R.A., Lindberg, F.A., Ryberg, P.T., 1983. Provenance of North American Phanerozoic sandstone in relation to tectonic setting. Geological Society of American Bulletin 94, 222–235.

Fedo, C.M., Sircombe, K.N., Rainbird, R.H., 2003. Detrital zircon analysis of the sedimentary record. In: Hanchar, J.M., Hoskin, P.W.O. (Eds.), Zircon, Reviews in Mineralogy and Geochemistry, 53, pp. 277–303.

Folk, R.L., Andrews, P.B., Lewis, D.W., 1970. Detrital sedimentary rock classification and nomenclature for use in New Zealand. New Zealand Journal of Geology and Geophysics 13, 937–968.

Franzese, J.R., 1995. El Complejo Piedra Santa (Neuquén, Argentina): parte de un cinturón metamórfico neopaleozoico del Gondwana suroccidental. Revista Geológica de Chile 22 (2), 193–202.

Franzese, J.R., Spalletti, L.A., 2001. Late Triassic–early Jurassic continental extension in southwestern Gondwana: tectonic segmentation and pre-break-up rifting. Journal of South American Earth Sciences 14, 257–270.

Franzese, J.R., Veiga, G.D., Schwarz, E., Gómez-Pérez, I., 2006. Tectono-stratigraphic evolution of a Mesozoic graben border system: the Chachil depocentre, southern Neuquén Basin, Argentina. Journal of the Geological Society of London 163, 207–221.

Franzese, J.R., Veiga, G.D., Muravchik, M., Ancheta, D., D'Elia, L., 2007. Estratigrafía de sin-rift de la Cuenca Neuquina en la Sierra de Chacaico, Neuquén; República Argentina. Revista Geológica de Chile. Servicio Nacional de Geología y Minería de Chile 34 (1), 49–62 2007.

García Morabito, E., 2010. Tectónica y estructura del retroarco andino entre los 38°15' y los 40°00'S. Doctoral Thesis (unpublished), Facultad de Ciencias Exactas y Naturales, Universidad de Buenos Aires, 284 pp.

García Morabito, E., Ramos, V.A., 2011a. La Precordillera Neuquina Sur en el contexto de los Andes Norpatagónicos. In: Leanza, H.A., Arregui, C., Carbone, O., Danieli, J.C., Vallés, J.M. (Eds.), Geología y Recursos Naturales de la Provincia de Neuquén. Relatorio del VXIII Congreso Geológico Argentino, Buenos Aires, pp. 355–365.

García Morabito, E., Goetze, H.J., Ramos, V.A., 2011b. Estudio integrado de un segmento del retroarco andino comprendido entre los 38°15' y los 40°00'S. Simposio de Tectónica Andina. XVIII Congreso Geológico Argentino, Neuquén.

García Morabito, E., Götze, H.J., Ramos, V.A., 2011. Tertiary tectonics of the Patagonian Andes retro-arc area between 38°15′ and 40°00′S latitude. Tectonophysics 499, 1–21.

Ghazi, S., Mountney, N.P., 2011. Petrography and provenance of the Early Permian Fluvial Warchha Sandstone, Salt Range, Pakistan. Sedimentary Geology 233, 88–110.

Goodge, J., Williams, I., Myrow, P., 2004. Provenance of Neoproterozoic and lower Paleozoaoic siliciclastic rocks of the central Ross orógeno, Antarctica: detrital record of rift-, passive- and active-margin sedimentation. Geological Society of America Bulletin 116 (9–10), 1253–1279.

Grimaldi, G.O., Dorobek, S.L., 2011. Fault framework and kinematic evolution of inversion structures: natural examples from the Neuquén Basin, Argentina. American Association of Petroleum Geologists Bulletin 9 (1), 27–60.

Groeber, P., 1946. Observaciones geológicas a lo largo del meridiano 70. 1. Hoja Chos Malal. Revista de la Sociedad Geológica Argentina 1 (3), 177–208.

Gulisano, C.A., 1988. Análisis estratigráfico y sedimentológico de la Formación Tordillo en el oeste de la Provincia del Neuquén, Cuenca Neuquina, Argentina. Doctoral Thesis (unpublished), Facultad de Ciencias Exactas y Naturales, Universidad de Buenos Aires, 235 pp.

Gulisano, C.A., Gutiérrez Pleimling, A.R., 1995. Field guide: the Jurassic of the Neuquén Basin. a) Neuquén province. Asociación Geológica Argentina, Serie E (2), 1–111 Buenos Aires.

Gulisano, C.A., Gutiérrez Pleimling, A.R., Digregorio, R.E., 1984. Esquema estratigráfico de la secuencia jurásica del oeste de la Provincia de Neuquén. IX Congreso Geológico Argentino, Actas 1, 236–259.

Howell, J.A., Schwarz, E., Spalletti, L.A., Veiga, G.D., 2005. The Neuquén Basin: an overview. In: Veiga, G.D., Spalletti, L.A., Howell, J.A., Schwarz, E. (Eds.), Geological Society, London, Special Publications 252, pp. 1–14.

Ingersoll, R.V., 1979. Evolution of the Late Cretaceous forearc basin, northern and central California. Geological Society of American Bulletin 96, 813–826.

Jaillard, E., Soler, P., Carlier, C., Mourier, T., 1990. Geodynamic evolution of the northern and central Andes during the middle Mesozoic times: a Tethyan model. Journal of the Geological Society 147, 1009–1022.

Leanza, H.A., 1981. The Jurassic–Cretaceous boundary beds in West Central Argentina and their ammonite zones. Neues Jahrbuch für Geologie und Paläontologie, Abhandlungen 161 (1), 62–92.

Leanza, H.A., 1990. Estratigrafía del Paleozoico y Mesozoico anterior a los Movimientos Intermálmicos en la comarca del cerro Chachil, provincia del Neuquén. Revista de la Asociación Geológica Argentina 45 (3–4), 272–299.

Leanza, H.A., 1993. Estratigrafía del Mesozoico posterior a los Movimientos Intermálmicos en la comarca del Cerro Chachil, provincia del Neuquén. Revista de la Asociación Geológica Argentina 48 (1), 71–84.

Leanza, H.A., 2009. Las principales discordancias del Mesozoico de la Cuenca Neuquina según observaciones de superficie. Revista del Museo Argentino de Ciencias Naturales 11 (2), 145–184.

Leanza, H.A., Hugo, C., 1997. Hoja Geológica 3969-III. Picún Leufú. Provincias de Neuquén y Río Negro. Servicio Geológico Minero Argentino, Boletín 218 135 pp., Buenos Aires.

Leanza, H.A., Llambías, E.J., Carbone, O., 2005. Unidades estratigráficas limitadas por discordancias en los depocentros de la cordillera del Viento y la sierra de Chacaico durante los inicios de la Cuenca Neuquina. V Congreso de Exploración y Desarrollo de Hidrocarburos, Trabajos Técnicos. CD-ROM.

Legarreta, L., Gulisano, C.A., 1989. Análisis estratigráfico secuencial de la Cuenca Neuquina (Triásico superior-Terciario inferior, Argentina). In: Chebli, G., Spalletti, L. (Eds.), Cuencas Sedimentarias Argentinas. : Serie Correlación Geológica, 6. Universidad Nacional de Tucumán, pp. 221–243.

Llambías, E.J., Kleiman, L.E., Salvarredi, J.A., 1993. El magmatismo Gondwánico. XVII Congreso Geológico Argentino y II Congreso de Exploración de Hidrocarburos. In: Ramos, V.A. (Ed.), Geología y Recursos Naturales de Mendoza, Relatorio I, 6, pp. 53–64. Buenos Aires.

Lucassen, F., Trumbull, R., Franz, G., Creixell, C., Vásquez, P., Romer, R.L., Figueroa, O., 2004. Distinguishing crustal recycling and juvenile additions at active continental margins: the Paleozoic to Recent compositional evolution of the Chilean Pacific margin (36–41°S). Journal of South American Earth Sciences 17, 103–119.

Marchese, H.G., 1971. Litoestratigrafía y variaciones faciales de las sedimentitas mesozoicas de la Cuenca Neuquina, provincia de Neuquén, República Argentina. Revista de la Asociación Geológica Argentina 26 (3), 343–410.

Morton, A.C., Hallsworth, C.R., 1999. Processes controlling the composition of heavy mineral assemblages in sandstones. Sedimentary Geology 124, 3–29.

Mosquera, A., 2008. Mecánica de deformación de la Cuenca Neuquina (Triásico-Terciario). Doctoral Thesis (unpublished), Facultad de Ciencias Exactas y Naturales, Universidad de Buenos Aires, 270 pp.

Mosquera, A., Ramos, V.A., 2006. Intraplate deformation in the Neuquén Embayment. In: Kay, S.M., Ramos, V.A. (Eds.), Evolution of an Andean margin: a tectonic and magmatic view from the Andes to the Neuquén Basin (35°–39° lat): Geological Society of America Special Paper 407, pp. 97–124.

Mosquera, A., Silvestro, J., Ramos, V.A., Alarcón, M., Zubiri, M., 2011. La estructura de la Dorsal de Huincul. In: Leanza, H.A., Arregui, C., Carbone, O., Danieli, J.C., Vallés, J.M. (Eds.), Geología y recursos naturales de la provincia de Neuquén. Relatorio del XVIII Congreso Geológico Argentino, pp. 385–397. Buenos Aires.

Mueller, P.A., Heatherington, A.L., Wooden, J.L., Shuster, R.D., Nutman, A.P., Williams, I.S., 1994. Precambrian zircons from the Florida basement: a Gondwana connection. Geology 22, 119–122.

Ogg, J.G., 2004. The Jurassic Period. In: Gradstein, F., Ogg, J., Smith, A. (Eds.), A Geologic Time Scale. Cambridge University Press, pp. 307–343.
Orchuela, I.A., Ploszkiewicz, J.V., Viñes, R., 1981. Reinterpretación estructural de la denominada "Dorsal Neuquina". VIII Congreso Geológico Argentino, Actas 3, 81–293.
Pángaro, F., Veiga, R., Vergani, G., 2002. Evolución tecto-sedimentaria del área de Cerro Bandera, Cuenca Neuquina, Argentina. V Congreso de Exploración y Desarrollo de Hidrocarburos. CD-ROM, 16 pp.
Pángaro, F., Pereira, D.M., Raggio, F., Pioli, O., Silvestro, J., Zubiri, M., Gozalvez, G., 2006. Tectonic inversion of the Huincul High, Neuquén Basin, Argentina: an endangered species. Stratigraphic evidences of it's disappearance. IX Simposio Bolivariano de Exploración Petrolera en Cuencas Subandinas (Cartagena), Actas. 9 pp.
Pángaro, F., Pereira, D.M., Micucci, E., 2009. El sinrift de la Dorsal de Huincul, Cuenca Neuquina: evolución y control sobre la estratigrafía y estructura del área. Revista de la Asociación Geológica Argentina 65 (2), 265–277.
Parker, G., 1965. Relevamiento geológico en escala 1:25000 entre el arroyo Picún Leufú y Catan Lil, a ambos lados de la ruta nacional N° 40. Informe Yacimientos Petrolíferos Fiscales , Buenos Aires.
Ploszkiewicz, J.V., Orchuela, I.A., Vaillard, J.C., Viñes, R., 1984. Compresión y desplazamiento lateral en la zona de la Falla Huincul, estructuras asociadas. Provincia del Neuquen. IX Congreso Geológico Argentino,Actas 2, 163–169.
Ramos, V.A., 2008. Patagonia: a Paleozoic continent adrift? Journal of South American Earth Sciences 26, 235–251.
Ramos, V.A., 2010. The tectonic regime along the Andes: present-day and Mesozoic regimes. Geological Journal 45, 2–25.
Ramos, V.A., García Morabito, E., Hervé, F., Fanning, C.M., 2010. Grenville-age sources in Cuesta de Rahue, northern Patagonia: constrains from U–Pb/SHRIMP ages from detrital zircons. International Geological Congress on the Southern Hemisphere. Bollettino de Geofisica 51, 42–44.
Rapela, C.W., Spalletti, L., Merodio, J., 1983. Evolución magmática y geotectónica de la "Serie Andesitica" andina (Paleoceno-Eoceno) en la Cordillera Norpatagónica. Revista de la Asociación Geológica Argentina 38, 469–484.
Rapela, C.W., Dias, G., Franzese, J., Alonso, G., Benvenuto, A., 1991. El Batolito de la Patagonia Central: evidencias de un magmatismo triásico-jurásico asociado a fallas transcurrentes. Revista Geológica de Chile 18, 121–138.
Rapela, C.W., Pankhurst, R.J., Fanning, C.M., Hervé, F., 2005. Pacific subduction coeval with the Karoo mantle plume: the early Jurassic Subcordilleran belt of northwestern Patagonia. In: Vaughan, A.P.M., Leat, P.T., Pankhurst, R.J. (Eds.), Terrane Processes at the Margins of Gondwana: Geological Society of London Special Publications 246, pp. 217–239.
Repol, D., 2006. Structural geology and tectonics in the southern extent of the Agrio Fold and Thrust belt, Neuquén Basin, Argentina. MSc. Thesis, Department of Geology and Geophysics, University of Calgary, 180 pp.
Riccardi, A.C., 2008a. The marine Jurassic of Argentina: a biostratigraphic framework. Episodes 31 (3), 326–335.
Riccardi, A.C., 2008b. El Jurásico de la Argentina y sus amonites. Revista de la Asociación Geológica Argentina 63 (4), 625–643.
Rosenau, M., 2004. Tectonics of the Southern Andean intra-arc zone (38°-42°S). Doctoral Thesis, Berlin, Germany, Free University, 159 pp.
Scheuber, E., Bogdanic, T., Jensen, A., Reutter, K.-J., 1994. Tectonic development of the North Chilean Andes in relation to plate convergence and magmatism since the Jurassic. In: Reutter, K.-J., Scheuber, E., Wigger, P.J. (Eds.), Tectonics of the Southern Central Andes: Structure and evolution of an active continental margin. Springer-Verlag, Berlin, pp. 121–139.
Schiuma, M., Llambías, E.J., 2008. New ages and chemical analysis on Lower Jurassic volcanism close to the Huincul High, Neuquén. Revista de la Asociación Geológica Argentina 63 (4), 644–652.
Sillitoe, R., 1977. Permo-Carboniferous–Upper Cretaceous and Miocene porphyry copper type mineralization in the Argentinean Andes. Economic Geology 72, 99–109.
Silvestro, J., Zubiri, M., 2008. Convergencia oblicua: modelo estructural alternativo para la Dorsal Neuquina (39°S)–Neuquén. Revista de la Asociación Geológica Argentina 63 (1), 49–64.
Spalletti, L.A., Colombo, Piñol F., 2005. From alluvial fan to playa: an Upper Jurassic ephemeral fluvial system, Neuquén Basin, Argentina. Gondwana Research 8, 363–383.
Spalletti, L.A., Queralt, I., Matheos, S.D., Colombo, F., Maggi, J., 2008. Sedimentary petrology and geochemistry of siliciclastic rocks from the upper Jurassic Tordillo Formation (Neuquén Basin, western Argentina): implications for provenance and tectonic setting. Journal South American Earth Sciences 25, 440–463.
Storti, F., Holdsworth, R.E., Salvini, F., 2003. Intraplate strike-slip deformation belts. Geological Society, Special Publication 210 1–234 London.
Teyssier, C., Tikoff, B., Markley, M., 1995. Oblique plate motion and continental tectonics. Geology 23 (5), 447–450.
Tikoff, B., Teyssier, C., 1994. Strain modeling of displacement-field partitioning in transpressional orogens. Journal of Structural Geology 16 (11), 1575–1588.
Tunik, M., Folguera, A., Naipauer, M., Pimentel, M.M., Ramos, V.A., 2010. Early uplift and orogenic deformation in the Neuquén Basin: constraints on the Andean uplift from U–Pb and Hf isotopic data of detrital zircons. Tectonophysics 489 (1–4), 258–273.
Turner, J.C., 1973. Descripción de la Hoja 37 a-b, Junín de los Andes, provincia del Neuquén. Servicio Nacional Minero Geológico, Boletín 138, 1–86 Buenos Aires.
Uliana, M., Arteaga, M., Legarreta, L., Cerdan, J., Peroni, G., 1995. Inversion structures and hydrocarbon occurrence in Argentina. In: Buchanan, J., Buchanan, P. (Eds.), Basin inversion, Geological Society, London, Special Publication 88, pp. 211–233.
Vergani, G., 2005. Control estructural de la sedimentación Jurásica (Grupo Cuyo) en la Dorsal de Huincul, Cuenca Neuquina, Argentina. Modelo de falla lístrica rampa-plano, invertida. Boletín de Informaciones Petroleras 1 (1), 32–42.
Vergani, G.D., Tankard, A.J., Belotti, H.J., Welsink, H.J., 1995. Tectonic evolution and paleogeography of the Neuquén Basin, Argentina. In: Tankard, A.J., Suárez Soruco, R., Welsink, H.J. (Eds.), Petroleum Basins of South America: American Association of Petroleum Geologists, Memoirs, 62, pp. 383–402.
Vietor, T., Echtler, H., 2006. Episodic Neogene southward growth of the Andean subduction orogen between 30° S and 40° S—plate motions, mantle flow, climate, and upper-plate structure. In: Oncken, O., Chong, G., Franz, G., Giese, P., Götze, H.-J., Ramos, V.A., Strecker, M.R., Wigger, P. (Eds.), The Andes—active subduction orogeny, Frontiers in Earth Science Series 1. Springer-Verlag, Berlin Heidelberg New York, pp. 375–400.
Zamora Valcarce, G., Zapata, T., Del Pino, D., Ansa, A., 2006. Structural evolution and magmatic characteristics of the Agrio Fold-and-thrust belt. In: Kay, S.M., Ramos, V.A. (Eds.), Evolution of an Andean margin: a tectonic and magmatic view from the Andes to the Neuquén Basin (35°–39° lat): Geological Society of America, Special Paper 407, pp. 125–145.
Zavala, C., Freije, H., 2002. Cuñas clásticas jurásicas vinculadas a la Dorsal de Huíncul. Un ejemplo del área de Picún Leufú. V Congreso de Exploración y Desarrollo de Hidrocarburos, Cuenca Neuquina. Argentina. CD-ROM.
Zavala, C., Maretto, H., Di Meglio, M., 2005. Hierarchy of bounding surfaces in Aeolian sandstones of the Tordillo Formation (Jurassic). Neuquén Basin, Argentina. Geologica Acta 3, 133–145.
Zavala, C., Martínez Lampe, J.M., Fernández, M., Di Meglio, M., Arcuri, M., 2008. El diacronismo entre las Formaciones Tordillo y Quebrada del Sapo (Kimeridgiano) en el sector sur de la cuenca neuquina. Revista de la Asociación Geológica Argentina 63 (4), 754–765.
Ziegler, P.A., Cloetingh, S., van Wees, J.-D., 1995. Dynamics of intra-plate compressional deformation: the Alpine foreland and other examples. Tectonophysics 252, 7–59.
Ziegler, P.A., van Wees, J.-D., Cloetingh, S., 1998. Mechanical controls on collision-related compressional intraplate deformation. Tectonophysics 300, 103–129.
Zonenshayn, L.P., Savostin, L.A., Sedov, A.P., 1984. Global paleogeodynamic reconstructions for the last 160 million years. Geotectonics 18 (3), 48–59.